Reports of the Department of Geodetic Science

Report No. 230

ERROR ANALYSIS FOR THE PROPOSED CLOSE GRID GEODYNAMIC SATELLITE MEASUREMENT SYSTEM (CLOGEOS)

by

Ivan I. Mueller, B. H. W. van Gelder and M. Kumar

Prepared for

National Aeronautics and Space Administration
George C. Marshall Space Flight Center
Huntsville, Alabama 35812

Contract No. NAS 8-31195
OSURF Project No. 4105-A1

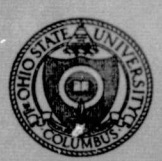

The Ohio State University
Research Foundation
Columbus, Ohio 43212

September, 1975

PREFACE

This project is under the supervision of Professor Ivan I. Mueller, Department of Geodetic Science, The Ohio State University and is under the technical direction of Dr. Nicholas Costes, Code ES31, NASA/MSFC, Huntsville, Alabama. The contract was issued by Procurement Office, MSFC, and is administered through the Office of Naval Research Resident Representative, Columbus, Ohio.

TABLE OF CONTENTS

1. INTRODUCTION

The Close Grid Geodynamic Measurement System experiment at The Ohio State University envisages an active ranging satellite and a grid of retro-reflectors or transponders in the San Andreas fault area and is a detailed simulated study for recovering the relative positions in the grid.

The San Andreas fault system in California and Mexico forms the boundary between the North American and the Pacific plates. The rate of opening in the Gulf of California appears to be 6 cm/year, but estimates of the rate of slip on the San Andreas fault system north of the transverse ranges vary from 1 to 6 cm/year [Drake et al., 1973]. Seismically, the system extends to the eastern margin of the Great Basin and along the Rio Grande depression. The importance of the area demands extremely accurate determination of the "relative" motion of the two large plates.

The Close Grid Geodynamic Measurement System for determining the relative motion of two plates in the California region, once experimented and found feasible, could then be used in other areas of the world to delineate and complete the picture of crustal motions over the entire globe and serve as a novel geodetic survey system. In addition, with less stringent accuracy standards, the system would also find usage in allied geological and marine geodesy fields (Table 1-1). Thus, in this role the system would then become complementary to the global Laser Geodynamic Satellite (Lageos) and other Earth and Ocean Dynamics Applications Program (EODAP) satellite systems.

As envisaged today there seem to be two main instrument concepts, viz., laser or radio frequency radar systems which will be available for inclusion

Table 1-1

Typical Requirements for Potential Close Grid Geodynamic Measurement System Applications
(MSFC Assessment, 1975)

POTENTIAL APPLICATION	ACCURACY (cm)	FREQUENCY	GRID SPACING (km)
DILATANCY	≤ 1	QUARTERLY	1-10
POST-GLACIAL UPLIFT	1-2	YEARLY	10
GEODETIC SURVEYS		YEARLY	10-50
SURFACE MOTIONS NEAR PLATE BOUNDARIES		QUARTERLY	10
REGIONAL STRAIN MEASUREMENTS		QUARTERLY	10-50
SUBSIDENCE	2-5	QUARTERLY	1-10
SURFACE MOTIONS OF CENTRAL REGIONS OF LARGE ICE CAPS		SEMI-ANNUALLY	10-50
UNSTABLE SLOPE MONITORING		WEEKLY TO YEARLY	0.5-10
VELOCITY FIELDS OF SURFACE IN MAJOR ICE SHEETS	5-10	MONTHLY	10-50
SURFACE MOTIONS IN PERMAFROST		WEEKLY TO MONTHLY	1-10
GLACIER FLOW VELOCITY FIELDS		WEEKLY TO MONTHLY	0.5-10
REGIONAL LAND BOUNDARY DEMARCATION		ONCE	10
LOCATION OF STATIONARY BUOYS	10-100	QUARTERLY	SAME DEPTH TO OCEAN BOTTOM
STRAIN MEASUREMENTS OF PACK ICE	100-1000	WEEKLY TO MONTHLY	1-10
OFF-SHORE BOUNDARY DEMARCATION		YEARLY	10
NAVIGATION		CLUSTER OF OBSERVATIONS	50
POSITIONING OF LARGE SEA-ICE SHEETS, ICE ISLANDS	1000	DAILY TO WEEKLY	SAME AS DEPTH TO OCEAN BOTTOM

Table 1-2

Instrument Concepts/Systems

	LASER RADAR		RF RADAR		COMBINATION	
	CW	PULSE	CW	PULSE	CW	PULSE
MEASUREMENT TECHNIQUES						
-DIRECT RANGE	X	X	X	X	X	X
-RANGE RATE (DOPPLER)	X	X	X	X	X	X
-INTEGRATED DOPPLER	X	X	X	X	X	X
TARGET ACQUISITION						
-WIDE BEAM (SPACECRAFT POINTING IS ADEQUATE)		X	X	X	X	X
-NARROW BEAM (GIMBALLED MIRROR OR SCANNING BEAM)	X	X			X	X
GROUND STATION						
-CUBE CORNER REFLECTORS	X	X			X	X
-ACTIVE TRANSPONDER			X	X	X	X

in the Close Grid Geodynamic Measurement System. Table 1-2 gives the specifications and nature of ground stations required by each system. However, if the Close Grid Dynamic Measurement System is to become feasible, the present state of system limitations for laser (5-10 cm) and/or radio frequency (100 cm) will require significant improvements.

What is needed then is a tool for making exceedingly accurate measurements from an active satellite to a grid of inexpensive (and passive) stations on the earth in a short span of time. Because of the brevity in time span for observations, it is important to assume that the observed grid stations do not move during that period. In order to make the system economically feasible and periodically repeatable, when the satellite is up and the observations cycle has been started it is imperative that the grid stations must be extremely simple requiring the least possible manual operations and maintenance.

In an observational campaign during any calendar period, the satellite will be activated to make accurate range measurements to the grid stations, identify each observation and transfer the requisite observational information to a data bank for subsequent data analysis; and this procedure then can be repeated periodically.

To meet the above considerations, the present simulated experiment assumes that the satellite has the capability of making accurate range measurements, either individually or collectively to grid stations, of identifying each observation, of noting the exact time of such observations and of transferring the information to a data bank.

2. APPROACHES TO DATA ANALYSIS

In the simplest case, when a (spherical) satellite moves around its (spherical) primary in an orbit affected only by the latter's attraction, the resulting normal orbit can be defined by six constants, E_i ($i = 1, 2 \ldots 6$). These parameters may be selected according to various theoretical and/or computational criteria. From a didactic point of view, the simplest set is the classical Keplerian elements, which define the orientation of the plane of the orbit in space (two parameters); the size, shape and orientation of the Keplerian ellipse in that plane (three parameters) and finally, the position of the satellite at some given epoch (one parameter). In the gravitational force field of the spherical primary these elements are constant and the satellite moves in its defined orbit in accordance with the laws of Kepler.

The circumstances of a near-earth artificial satellite are different from the above, the main consequence being that the orbital elements will no longer be time invariant, or in other words, their derivatives with respect to time, $\dot{E}_i$ ($i = 1, 2 \ldots 6$), will not be equal to zero. The variation of a given element from some reference epoch, T_0, to the epoch of utilization, T, can symbolically be described by the following equation:

$$E_i = E_i^0 + \int_{T_0}^{T} \dot{E}_i \, dT$$

where E_i^0 is the element in question at the epoch T_0, and E_i at T. The integral represents the perturbation of the element E_i. The function $\dot{E}_i$ is the rate of change of the element E_i due to all perturbing forces (nonspherical part of the earth's attraction, atmospheric drag, etc.) and as such is a function of several hundred parameters, P_j ($j = 1, 2 \ldots n$)

defining these forces. For example, an adequate description of the earth's gravitational field may require as many as 500, the atmospheric drag 10 and the radiation pressure 5 force parameters. The integral may be solved analytically (method of general perturbations) or numerically (method of special perturbations).

Once the orbital elements are thus computed at the epoch T, they can be readily converted into positional and velocity components of the satellite and referenced to some well-defined coordinate system. If the parameters defining the observer's position in this coordinate system, S_k (k = 1, 2, 3), are also known, the observables can be calculated, i.e., predicted. To refer the positions of the satellite and the observer to the same (usually earth-fixed) coordinate system, the precise knowledge of precession, nutation, polar motion and earth rotation (UT 1) is also required.

For principal geodetic results the observables are frequency (range rate), range, range difference and direction components (e.g., right ascension and declination), either observed individually or in certain combinations. Provided that the theory of motion, e.g., the mathematical model is correct and that the observations have been reduced to station and freed of systematic errors, the differences between the computed, C_ℓ (ℓ = 1, 2, ... m) and the observed O_ℓ values of the observables will be due to the erroneous geocentric coordinates of the observer S_k and the erroneous orbital elements, thus the parameters P_j. Assuming that both the differences $O_\ell - C_\ell$, and the errors dP_j, dS_k are differentially small, the following type of relations may be established:

$$O_\ell - C_\ell = \sum_j \frac{\partial C_\ell}{\partial P_j} dP_j + \sum_k \frac{\partial C_\ell}{\partial S_k} dS_k \qquad (1)$$

where

$$\frac{\partial C_\ell}{\partial P_j} = \frac{\partial C_\ell}{\partial E_i} \frac{\partial E_i}{\partial P_j} \qquad (2)$$

E_i being an orbital element at the instant of observation.

If equation (1) is regarded as an observation equation, the quantities dP_j and dS_k are the vector components representing the unknown corrections to the assumed parameters and station coordinates, respectively; and $\partial C_\ell / \partial P_j$ and $\partial C_\ell / \partial S_k$ are the elements of the corresponding coefficient of design matrices. In order to obtain a satisfactory solution, the number of observations (m) must greatly exceed the number of unknown parameters (n) plus the station unknowns p x k (p is the number of stations), and a least squares adjustment is performed in the traditional sense. To perform such a calculation is a formidable task considering that recent solutions, for example, included data from 10-20 satellites observed over 2-4 week periods from as many as 50-100 stations, and thus the unknowns included 150-300 components of positions in addition to the some 450-500 gravitational coefficients, thousands of orbital constants (e.g., E_i^0 - s), possibly pole position parameters, etc. Such general solutions, because of the high cost of forming the large normal equation matrices and of their inversions, are performed infrequently and only by a few organizations having access to large computers.

Once the results of a general solution such as the one outlined above are available, additional stations can be added on at a much smaller cost. In such partial solutions, positions of observing stations are obtained from least squares adjustments, where the earth's gravity field and the positions of many of the stations are held at values determined in the preceding general solution. Usually a separate computer program is used

for this purpose because program efficiency is greater when the objectives are more limited. In these solutions shorter time span of data (2-5 days) may be used, which will also reduce the effect of some errors in the force field. The unknowns in such a solution, in addition to the coordinates of the new stations, include the six initial orbital constants (E_i^0), usually a drag (scaling) parameter and maybe components of the pole position. In other words, in such solutions most perturbations are treated as known phenomena which can be calculated from the parameters determined in the general solution.

Two special cases of the partial solution are the so called short arc and the point positioning methods. In the former, the data is limited generally to satellite passes of 10-30 minute lengths. These relatively inexpensive solutions contain as unknowns only six initial orbital parameters per pass and the coordinates of participating stations. The method is limited to relative positioning with respect to a reference station whose coordinates are held to their estimated (not necessarily geocentric) values. Due to the shortness of the arc the perturbation models may be simpler than in the partial solutions; for example, the gravity field may be satisfactorily described by as few as 50-75 parameters, depending mainly on the length of the arc and the altitude of the satellite. The relative station positions obtained from short arc solutions are considered generally free of orbital (or other) biases equally affecting stations observing the same arcs.

In the point positioning method the data span is several (2-7) days long and the orbital elements are held to their values obtained from a precise satellite ephemeris. Thus the only unknowns in the solution are the coordinates of the observing stations. The satellite ephemeris is generated

and made available by some organization which keeps continuous track of the satellite(s) in question. A prime example of this method is positioning through the use of instruments which measure the range difference between a ground station and two satellite positions by means of integrating the Doppler shift of radio transmissions from the Navy Navigational Satellites. Precise ephemerides of these satellites are generated by the Naval Surface Weapons Center (formerly the Naval Weapons Laboratory) in Dahlgren, Virginia, from which satisfactory orbital elements may be obtained for the instants of the observations. Predicted, and therefore less accurate, elements are also generated and injected into the satellite's memory by the Naval Astronautics Group, Point Mugu, California, which in turn are retransmitted and can be used with certain types of receivers. In this latter case, it is advisable to observe the satellite passes from at least two stations simultaneously and solve only for relative positions which, similarly in the short arc case, will be less affected by the biases in the orbital elements than the positions themselves. This mode of operation is termed translocation.

In cases where simultaneous observations are made of the satellite from two or more stations, the satellite may be used only as the target of observations and the fact that it moves in an orbit can be ignored. The target, in fact, may as well be a rocket, a balloon, or an airplane carrying proper instrumentation, instead of being a satellite. The orbital elements E_i in equation (2) in this case become parameters and $\partial E_i / \partial P_j$ are identity matrices. After converting the parameters E_i to satellite-target coordinates, $T_k (k = 1, 2, 3)$, referenced to the same coordinate system in which the station coordinates S_k are sought, equation (1) will have the following form:

$$O_\ell - C_\ell = \sum_k \frac{\partial C_\ell}{\partial S_k} (dT_k - dS_k)$$

where, as before, the left side is the discrepancy between the observed and computed (predicted) values of the observables. In the right side, dT_k and dS_k are the unknown corrections to the predicted target and assumed station coordinates, respectively, and $\partial C_\ell / \partial S_k$ is the coefficient matrix.

In this mode of operation the observables at a given station have been mostly restricted to ranges (trilateration) or directions (triangulation) although range differences or a combination of ranges and directions can also be used.

In order to invert a system of geometric normal equations, a certain number of constraints will have to be introduced. These are due to the fact that while in the dynamic solutions the system to which the station coordinates refer is defined through satellite dynamics, in the geometric solutions it is not defined. Thus, in the case of satellite triangulation, when the satellite directions are determined from photographs against the background of stars, the orientation of the system is inherently defined by means of the star catalog used. The origin of the system is to be specified by holding three coordinates of a station to their a priori values and the scale is to be defined by constraining the distance between two stations to its measured value. Thus, in this case the minimum number of constraints to be introduced to obtain a solution is four. In the case of trilateration, only the scale is inherent in the observations; thus the origin and the orientation of the system are to be defined. This can be done, for example, by holding six coordinates distributed between three stations to their estimated values. In practice usually more than these minimum constraints are applied. They are usually available from accurate ground

survey information which may be included in the solution if their values are to be preserved. Such information may be the relative positions of neighboring stations, known distances between stations, heights, etc.

It should be mentioned at this point that the geometric mode is very sensitive to the problem of critical configurations. If the stations and/or the target points happen to be in such configurations with respect to each other, the solution will be singular even when the number of observations is sufficient and the coordinate system is properly defined. Near singularity or ill-conditioning will occur when the stations and/or the satellites are near the critical configurations. The problem has been well studied and methods of avoiding it for trilateration may be found in [Blaha, 1971b]; for triangulation in [Tsimis, 1972] and for range differences in [Tsimis, 1973].

2.1 Recovery of Station Coordinates

To determine the relative positions of the grid stations with the required accuracy, the geometric and short arc modes are the most promising. They have advantages and disadvantages with restrictions of different character on the data. One mode involves the geometry and its limiting critical degeneracies, while the other follows the orbital path with its complexities arising from modeling of the earth's potential field, atmospheric drag, radiation pressure, etc. The advantages and limitations of each mode are tabulated in Table 2.1-1.

Table 2.1-1

Advantages/Limitations of Geometric vs. Short Arc Mode

Geometric Mode	Short Arc Mode
Advantages	Advantages
1. No strict requirement for time of observation.	1. No requirement for simultaneous observations.
2. No dependence on orbital errors and geophysical assumptions.	2. Requires only six parameters per pass for satellite positions; hence lesser number of unknowns are involved.
3. System's overall accuracy is directly proportional to the observational accuracy.	3. Use of orbital constraints, i.e., the satellite follows an orbit, provides strength to the system.
Limitations	Limitations
1. Geometric configurations involving both stations and satellite points can be extremely CRITICAL.	1. Time of observations must be known accurately.
2. Minimum number of stations participating in an observational event is four (in a limited area it is six).	2. Requires at least two to three distant stations observing in any pass for coordinate system definition, i.e., for stability of solution.
3. Simultaneous observations are difficult to obtain.	3. Basic uncertainty in scale arising from uncertainties in fundamental parameters, such as GM, etc., is inherent.
4. Station positions obtained are relative.	

2.1.1 Geometric Mode

2.1.1.1 General Comments

The results in the geometric mode are determined from solutions through trigonometric computations based on simultaneous observations of a satellite from four or more ground stations (six in a limited area) [Blaha, 1971b;

Escobal et al., 1973]. The strength of the system lies in the fact that the error in satellite position in any event of simultaneous observations has very little influence on the overall accuracy of the system because these errors are more or less common to the observations from each of the stations participating in the event observation. Further, this impediment can be improved upon by using two or more satellite passes with "differing geometry" in the solution.

However, the system is highly sensitive to the configuration of both the stations and the targets (i.e., satellite positions) observed [Blaha, 1971b; Aardoom, 1972; Tsimis, 1973]. This sensitivity to "critical" configuration can be avoided (section 2.1.1.4) towards obtaining a near perfect recovery of the relative positions between the ground stations in the system.

2.1.1.2 Mathematical Modeling

The complete details of the theory involved can be found in [Krakiwsky and Pope, 1967; Mueller et al., 1970, and Mueller et al., 1973]. However, a brief development of the mathematical model is given below.

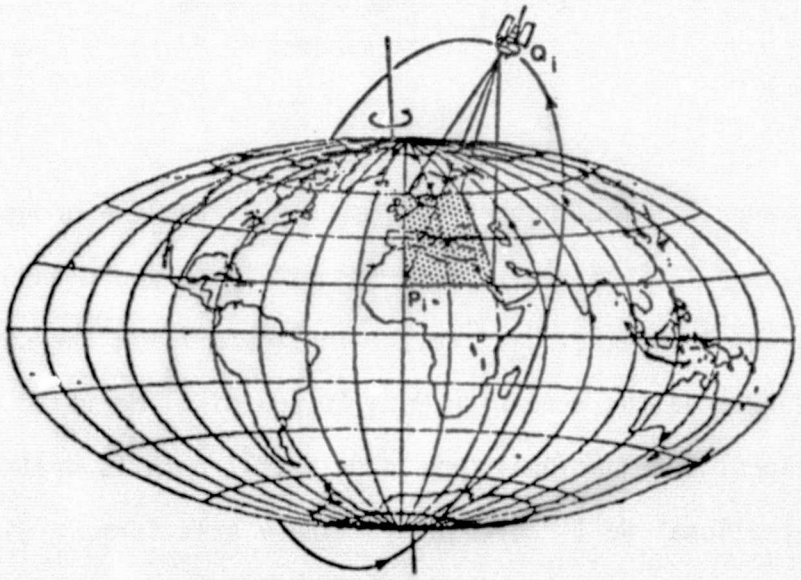

Fig. 2.1-1

Figure 2.1-1 shows a satellite in orbit around the earth and a typical footprint with four stations. For the range observations in geometric mode, each participating station (P_i) observes the distance (P_iQ_j) to the satellite position (Q_j) at an event (E_j, Q_j, $|t_j|$) (Figure 2.1-2).

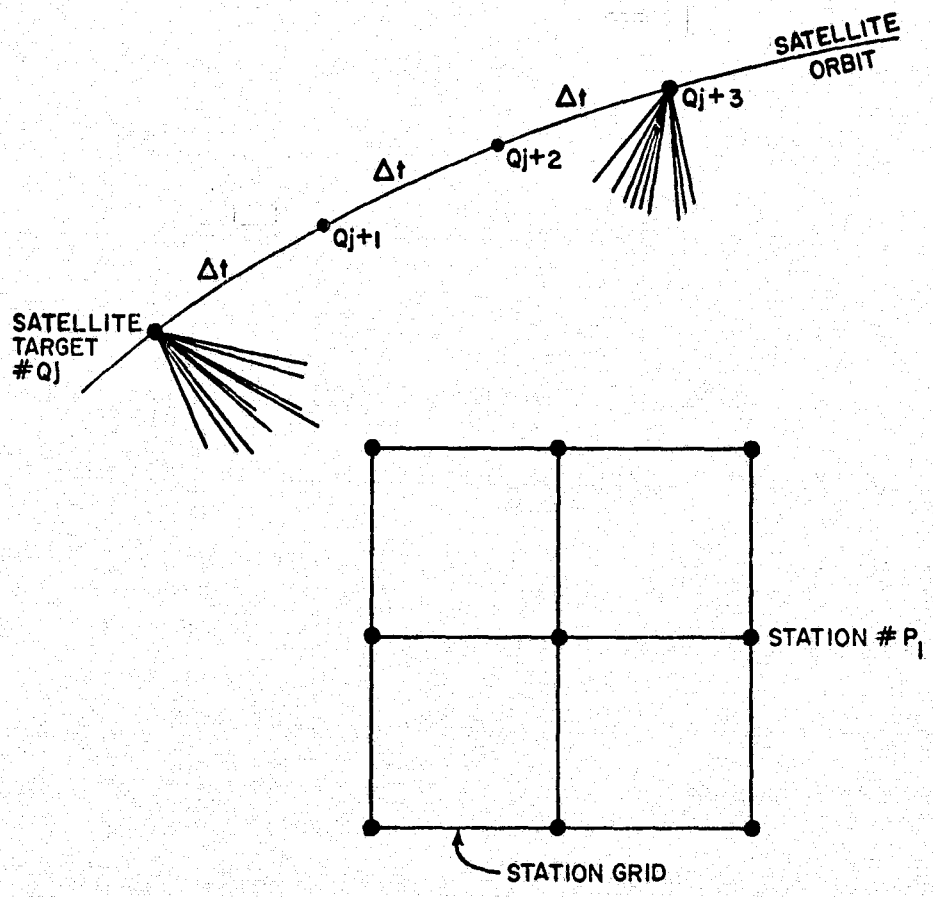

Fig. 2.1-2

This means that the topocentric range r_{ij} from the ground stations P_i (u_i, v_i, w_i; i = 1, 2, 3, 4, ...) to the satellite position Q_j (u_j, v_j, w_j) constitutes the event (E_j, Q_j, $|t_j|$). In Figure 2.1-3 the coordinate system is oriented towards the Greenwich Mean Astronomical Meridian (u axis) and the Conventional International Origin (w axis), both as defined by the Bureau International de l'Heure (BIH). The v axis forms a right-handed

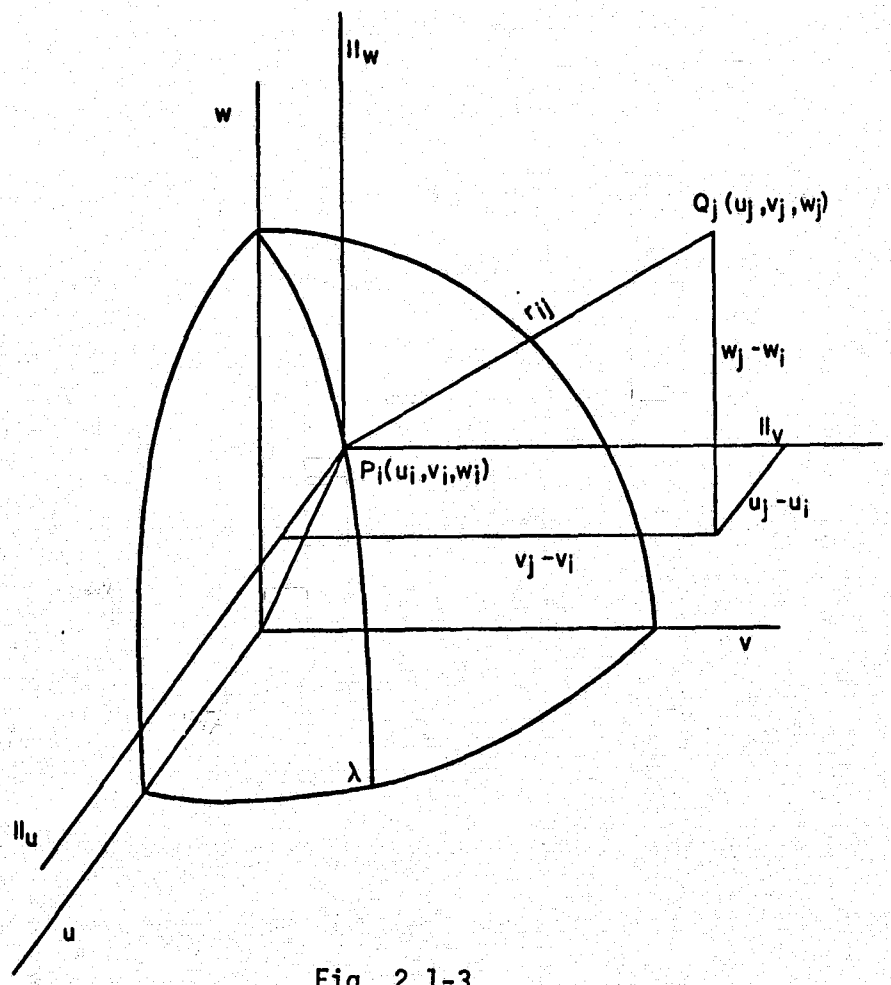

Fig. 2.1-3

system with u and w, and with u it defines the average geodetic equator. Thus, the mathematical model for any range r_{ij} can be written as

$$r_{ij} = [(u_j - u_i)^2 + (v_j - v_i)^2 + (w_j - w_i)^2]^{\frac{1}{2}} \qquad (3)$$

or

$$F_{ij} \equiv [(u_j - u_i)^2 + (v_j - v_i)^2 + (w_j - w_i)^2]^{\frac{1}{2}} - r_{ij} = 0 \qquad (4)$$

Equation (4) can then be linearized in the matrix notation [Uotila, 1967]:

$$BV + AX + W = 0 \qquad (5)$$

where

$$B_{ij} = \frac{\partial F_{ij}}{\partial r^{\circ}_{ij}} = [0 \mid -1 \mid 0];$$

$$A_{ij} = \frac{\partial F_{ij}}{\partial \vec{u}^{\circ}_{j},\ \partial \vec{u}^{\circ}_{i}} = [a_{ij} \mid -a_{ij}];$$

$$a_{ij} = \left[\frac{u^{\circ}_{j} - u^{\circ}_{i}}{r^{\circ}_{ij}} \quad \frac{v^{\circ}_{j} - v^{\circ}_{i}}{r^{\circ}_{ij}} \quad \frac{w^{\circ}_{j} - w^{\circ}_{i}}{r^{\circ}_{ij}}\right];$$

$$X_{ij} = [du_j\ dv_j\ dw_j \mid du_i\ dv_i\ dw_i]^T ;$$

$$W_{ij} = r^{\circ}_{ij}(\text{computed}) - r^{b}_{ij}(\text{observed}).$$

The values u°_{j}, u°_{i}, ... etc. are the initial approximate values which are used to compute approximate r°_{ij} from equation (3). The approximate satellite position $(u^{\circ}_{j}, v^{\circ}_{j}, w^{\circ}_{j})$ for any event results from a preliminary least squares adjustment for that event with observing stations held fixed [Krakiwsky and Pope, 1967]. The matrix B then becomes a negative unit matrix [-I] and the residual matrix V corresponds to the observed ranges r^{b}_{ij}.

Equation (5), after some mathematical manipulation in a least squares adjustment and elimination of nuisance parameters X_j, takes the form of the reduced normal equations [Mueller, 1967; Mueller, 1968]:

$$NX_j + U = 0 \qquad (6)$$

where the 3 x 3 blocks in N and 3 x 1 blocks in U are given as

$$N_{kk} = \sum_j a^T_{kj} p_{kj} a_{kj} - \sum_j a^T_{kj} p_{kj} a_{kj} \left[\sum_j a^T_{ij} p_{ij} a_{ij}\right]^{-1} a^T_{kj} p_{kj} a_{kj}$$

$$N_{k\ell} = -\sum_j \{a^T_{kj} p_{kj} a_{kj} \left[\sum_i a^T_{ij} p_{ij} a_{ij}\right]^{-1} a^T_{\ell j} p_{\ell j} a_{\ell j}\}$$

$$U_k = -\sum_j a^T_{kj} p_{kj} a_{kj}$$

In the above expressions, $\sum_i$ is the summation over all ground stations involved in event (E_j, Q_j, $|t_j|$) and $\sum_j$ over all events observed by ground stations k and/or ℓ.

2.1.1.3 Constraint's Contribution to the Normal Equation

The normal matrix as reached in the reduced normal equation (6) is "singular," i.e., the system still lacks the orientation and origin definitions while the requirement of scale is inherent in range measurements. This can be avoided, for example, by holding six coordinates distributed between any three stations in the system to any specified designated values. In practice, usually more constraints are applied than these minimum constraints. Details about the theoretical background of different types of constraints, effect of weights and their application/contribution to the normal equations can be found elsewhere [Mueller et al., 1973; Uotila, 1967].

However, even though the definition of a coordinate system is arbitrary in the case of a minimum constraint solution, the selection of six coordinates to be constrained in the case of ranging is very critical, since any one set of constraints would not give a unique solution. The statistics for any ground station coordinates in the system (other than the constrained coordinates) would be significantly different in each case depending upon varying propagation of errors.

To obviate this situation, the "best" solution is arrived at in a coordinate system defined through the use of a set of inner constraints [Rinner et al., 1969; Blaha, 1971a] where the trace of the variance-covariance matrix for the unknowns would be minimum compared to any other solution. The resulting adjustment is termed "free." The functional inner constraints for origin and orientation can be written as

$$C\,X = 0 \tag{7}$$

where

$$C \equiv \begin{bmatrix} C_1 \\ --- \\ C_2 \end{bmatrix} = \left[\begin{array}{ccc|ccc|c|c} \multicolumn{3}{c|}{I} & \multicolumn{3}{c|}{I} & & \\ \multicolumn{3}{c|}{3 \times 3} & \multicolumn{3}{c|}{3 \times 3} & & \\ \hline 0 & w_1^\circ & -v_1^\circ & 0 & w_2^\circ & -v_2^\circ & & \\ -w_1^\circ & 0 & u_1^\circ & -w_2^\circ & 0 & u_2^\circ & & \\ v_1^\circ & -u_1^\circ & 0 & v_2^\circ & -u_2^\circ & 0 & & \end{array}\right]$$

The number of 3 x 3 unit blocks is the same as total number of unknown points. Thus, combining equations (6) and (7), the resultant normal equation becomes [Blaha, 1971a]:

$$\begin{vmatrix} N & C^T \\ C & 0 \end{vmatrix} \begin{vmatrix} X \\ -K \end{vmatrix} + \begin{vmatrix} U \\ 0 \end{vmatrix} = 0 \tag{8}$$

where the a posteriori "weight coefficient" matrix Q_X for the unknown X is given as

$$Q_X = \{N + C^T [CC^T]^{-1} C\}^{-1} \{I - C^T[CC^T]^{-1}C\} = N^+$$

The above approach defines an optimal coordinate system where the adjusted coordinates preserve the mean positions and orientation of the initially adopted coordinates with no station or stations being preferred over any other station.

2.1.1.4 Critical Configuration

As stated earlier, if the ground stations and/or satellite points happen to be in critical configuration with respect to each other, the solution for the system will be singular even when the number of

observations is sufficient and the coordinate system is properly defined through requisite constraints. Blaha has discussed different cases of singularities and categorized them as singularities A, B, C [Blaha, 1971b] (see Figures 2.1-4 through 2.1-8).

In practice, the case of near singularity or ill conditioning also effects any solution and degenerates the recovery of the system when the stations and/or the satellite points are near critical case. Such cases are dangerous as the effects are, more or less, an inherent part of the solution and not distinguishable at all times. The problem has been well studied [Blaha, 1971b; Tsimis, 1972 and 1973] and Tables 2.1-2 and 2.1-3 summarize the methods of avoiding singular solutions.

A study of Tables 2.1-2 and 2.1-3 shows that in any system the degeneracy can be avoided either (1) through the introduction of height separation between the ground stations or (2) by observing satellite targets well distributed on at least two significantly different altitudes.

The first condition, within a limited area, obviously has its own topographical limitations: The inclusion of distant (several hundred km) stations is helpful in this regard. In the simulated experiment under report with general station separation of 7 - 10 km, and no distant stations, the best possible results were obtained when the targets were observed at 9 km and 1007 km altitudes. This introduces an extremely flexible and practical operational system where an airplane can be flown to obtain necessary and sufficient observations together with a satellite. It is not necessary that both types of targets be observed simultaneously.

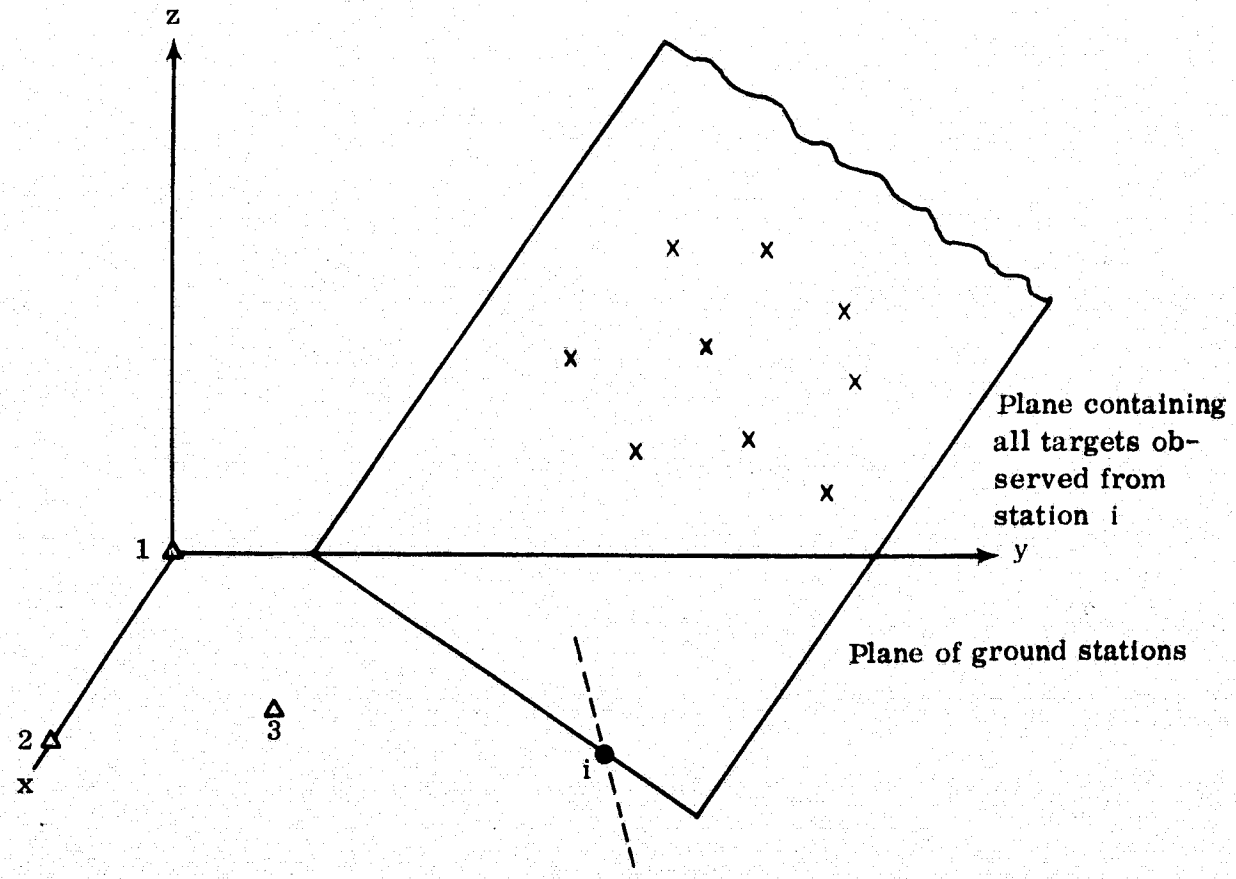

Figure 2.1-4

ILLUSTRATION OF SINGULARITY A): Station i is in the plane of its observed targets.

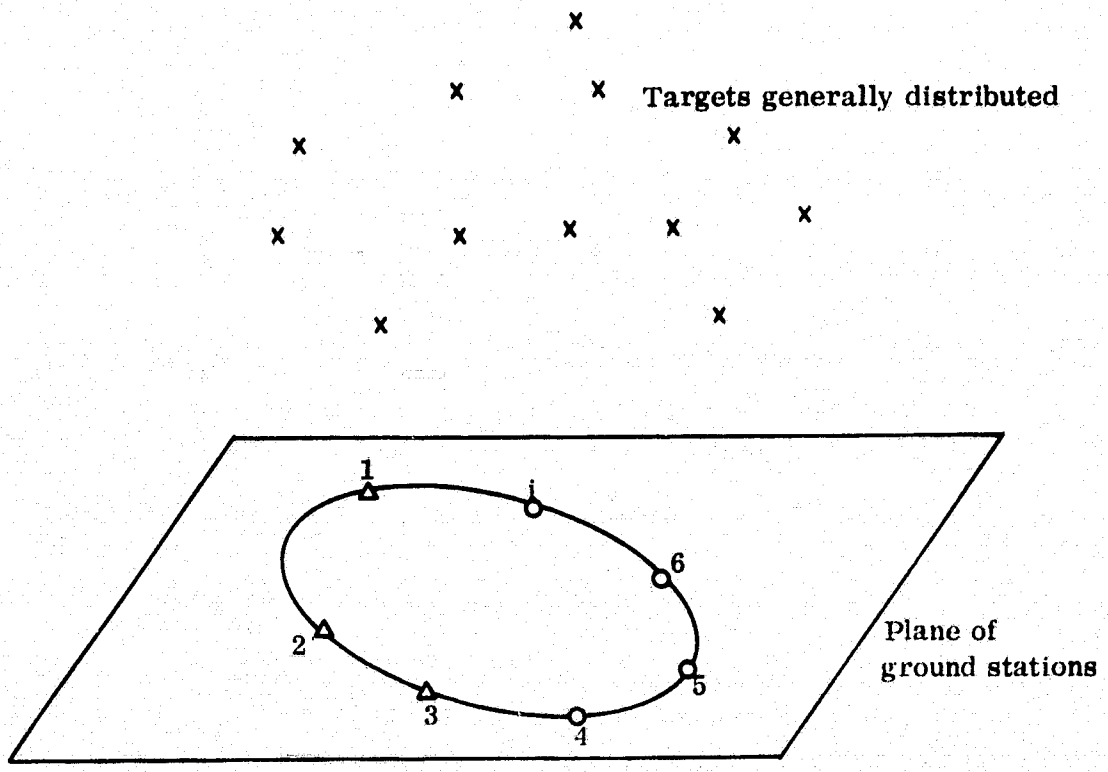

Figure 2. 1-5

ILLUSTRATION OF SINGULARITY B): Stations 1, 2, 3 observe all targets; all stations are on a second order curve.

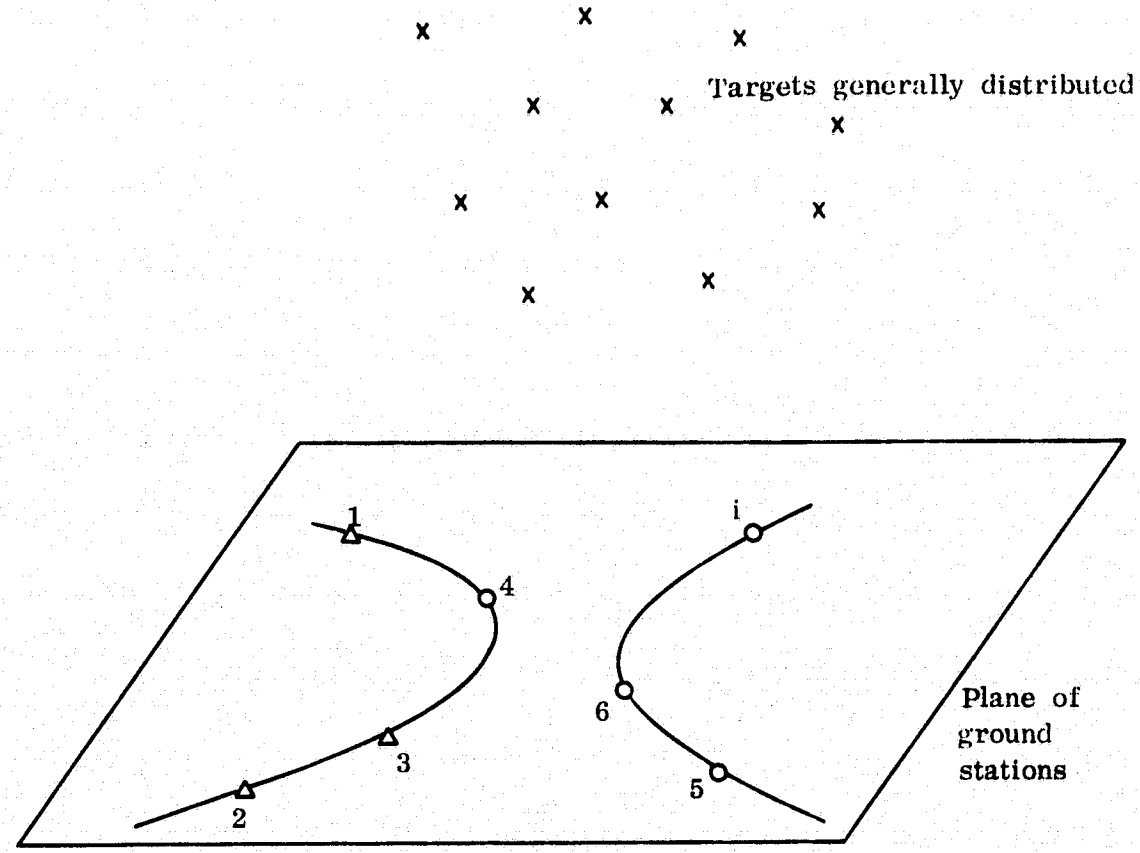

Figure 2.1-6

ILLUSTRATION OF SINGULARITY C): All stations observe all targets; all stations are on a second order curve.

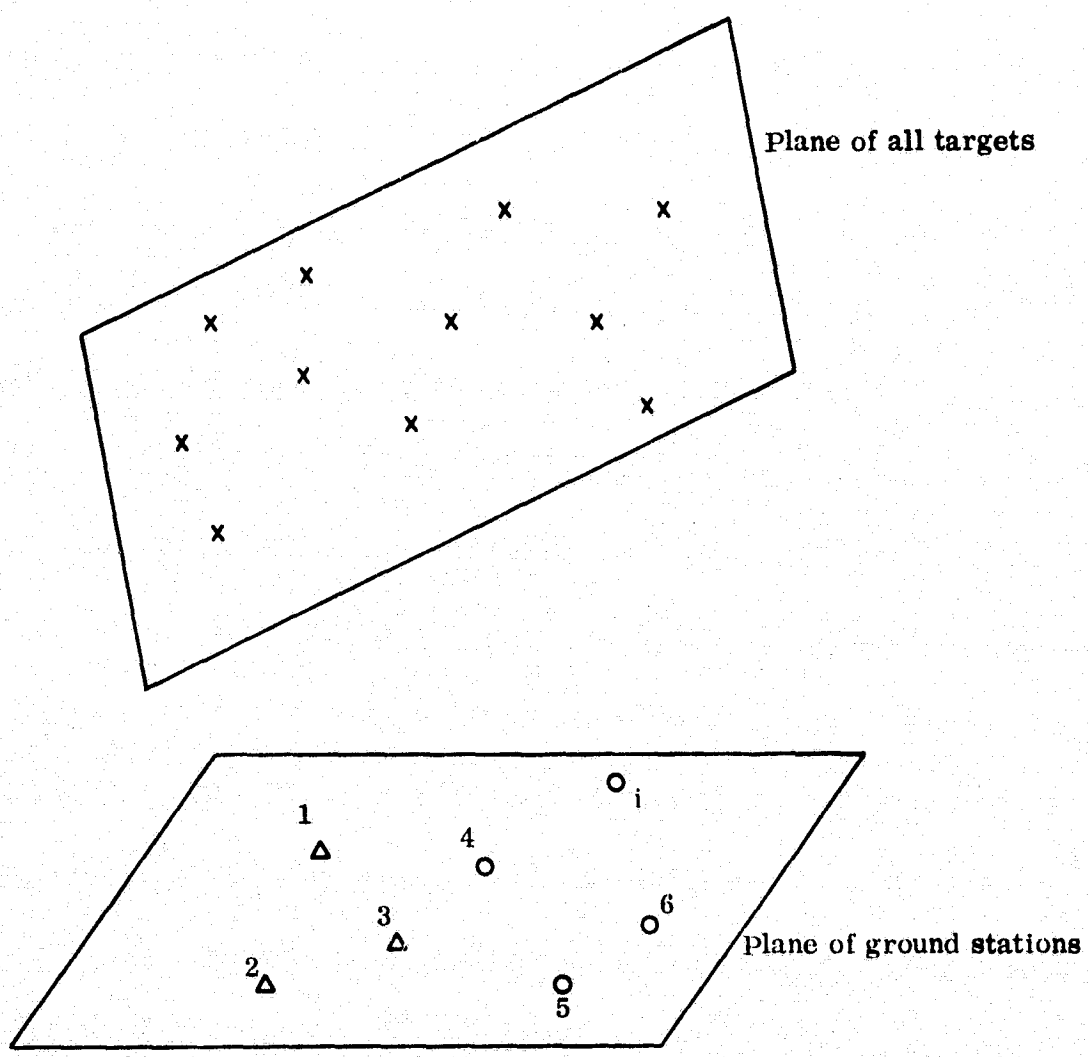

Figure 2.1-7

ILLUSTRATION OF SINGULARITY C): All stations observe all targets; all targets are in a plane.

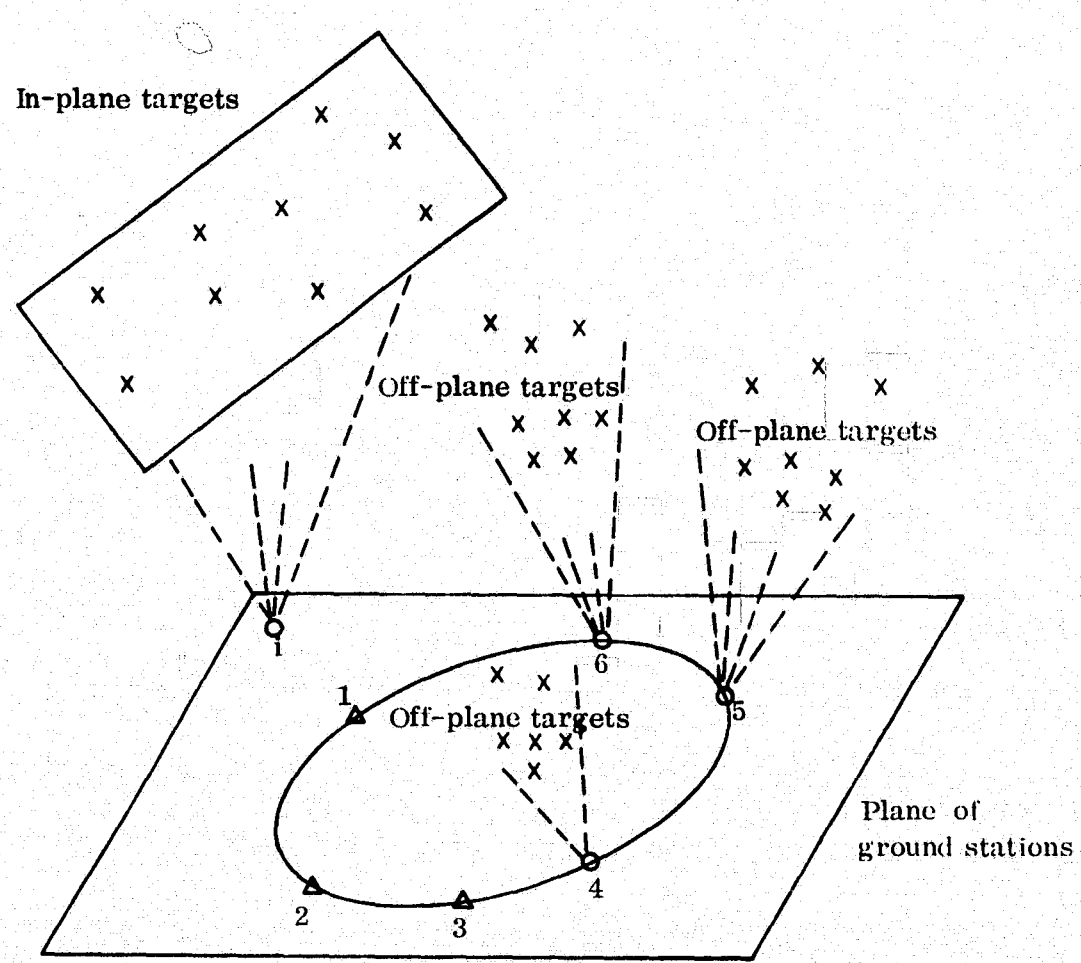

Figure 2.1-8

ILLUSTRATION OF SINGULARITY C): Stations 1, 2, 3 observe all targets; all stations observing off-plane targets are on a second order curve with stations 1, 2, 3.

Table 2.1-2

Necessary and Sufficient Conditions to Avoid Singular Solutions
When All Ground Stations Are in a Plane

Type of Singularity	Arrangement of Observations		Necessary Conditions to Prevent Singularity	Sufficient Conditions to Prevent Singularity	Note
Singularity A) (or closely related singularity)	Any		No station should be in a plane with all its observed targets (distributed over one or more satellite groups)	No station should be in a plane with the corresponding satellite group	This singularity is assumed non-existent in analysis of singularity C)
Singularity C) (global type of singularity)	Stations 1, 2, 3 observe all targets		Three stations in addition to 1, 2, 3 not lying on a second order curve with them should observe off-plane targets	The same as the necessary conditions	Special case of singularity C) is singularity B); it occurs when all stations are on a second order curve
	Station k replaces station 3 (satellite group j_4 contains off-plane targets)	Group j_k contains off-plane targets	One station in addition to 4 and k not lying on a second order curve with 1, 2, 3, 4, k should observe off-plane targets	The same as the necessary conditions	
		Group j_k contains in-plane targets	Two stations in addition to 4 should observe off-plane targets. Always: Avoid all stations lying on a second order curve	More complex requirements (according to stations which observe off-plane targets)	
	All stations observe all targets (all stations co-observe)		Avoid all targets lying in a plane (any plane) and all stations lying on a second order curve	The same as the necessary conditions	

Table 2.1-3

Necessary and Sufficient Conditions to Avoid Singular Solutions

When Ground Stations Are Generally Distributed

Type of Singularity	Arrangement of Observations	Necessary Conditions to Prevent Singularity	Sufficient Conditions to Prevent Singularity	Note
Singularity A) (or closely related singularity)	Any	No station should be in a plane with all its observed targets (distributed over one or more satellite groups)	No station should be in a plane with the corresponding satellite group	This singularity is assumed non-existent in analysis of global singularity
Reversed Singularity B)	Any	Targets should not be all in a plane on a second order curve	The same as the necessary conditions	This singularity is assumed non-existent in analysis of global singularity
Global Singularity	Stations 1, 2, 3 Observe all targets	Avoid all satellite groups (one group per quad) containing targets lying all on the corresponding second order critical surfaces (one surface per quad). Always: Avoid all points lying on a second order surface	The same as the necessary conditions	All the critical surfaces can be computed explicitly. They all intersect in the plane of stations 1, 2, 3 on a second order curve containing the three stations. If four points outside this plane are common to some critical surfaces then these surfaces coincide
	Station replacement (e.g., leapfrogging)	Always: Avoid all points lying on a second order surface	Avoid certain second order surfaces not expressed explicitly	
	All stations observe all targets (all stations coobserve)	Avoid all points lying on a second order surface	The same as the necessary conditions	

2.1.1.5 Computation of Estimable Quantities and Their Statistics

In most ranging systems a lack of coordinate system definition results in a design matrix A which is less than full column rank. In an ordinary least squares solution the rank of A is equal to the number of unknowns u, i.e., $R(A) = u$. As indicated earlier, if we assume that a ranging measurement system defines the scale, the system still lacks information about orientation (3 angles) and position (3 coordinates). This results in column rank of A which is six smaller than the number of unknowns, i.e., $R(A) = u - 6$.

The normal equations $(A^TA)X + U = 0$ cannot be solved for using the Caylean inverse since the determinant of the normal matrix N is equal to zero or $R(N) = R(A^TA) = R(A) = u - 6$. However, a unique solution for X can still be obtained using the pseudo inverse $X = -N^+ U$ (the least squares method using the pseudo inverse minimizes not only V^TPV, but also X^TX). But X is not a vector of estimable quantities, i.e., $E(X) \neq X$ [Grafarend and Schaffrin, 1974].

A method to compute the pseudo inverse N^+ is to border the singular matrix N by columns and/or rows which are orthogonal to all the columns and/or rows of the matrix N. The usual Caylean inverse can be computed now and from the inverse the added columns and/or rows are removed (transpose-wise). The resulting matrix is the pseudo inverse of the normal matrix N [Bjerhammer, 1973].

In case the rank deficiency of the matrix N is caused by a lack of coordinate system definition, the above-mentioned method of computing the pseudo inverse of N is known as the method of applying inner constraints

(see section 2.1.1.3). The added orthogonal rows and columns are the constraints added to the normal equations which yield a solution vector in the "best" coordinate system.

The disadvantage of this method, which was already mentioned earlier, is that it results in the nonestimable quantities $E(X) \neq X$.

A transformation R is needed to map the solution vector of nonestimable quantities X into a vector of estimable quantities X'

$$X' = RX.$$

In case of a range measurement system, the vector X consists of coordinates as obtained from the (pseudo inverse) inner constraint least squares solution. The vector X' (= RX) is said to be estimable if the following necessary and sufficient condition is fulfilled [Rao, 1973]:

$$R \{I - (A^T A)^+ (A^T A)\} = 0. \qquad (9)$$

This condition is fulfilled for the chords and angles between stations in case of a ranging measurement system, assuming that the scale is defined by the ranges themselves.

The variance/covariance matrix of X' is obtained the usual way:

$$"\Sigma"_X = (A^T A)^+ = N^+$$
$$\Sigma_{X'} = RN^+ R^T.$$

Thus in view of the above, the distances r_{ij} and the angles α_{ijk} between the stations i, j (and k) are the only estimable quantities when the geometric solutions are obtained with inner constraints. These quantities are defined as follows:

$$r_{ij} = \sqrt{(x_i - x_j)^2 + (y_i - y_j)^2 + (z_i - z_j)^2}$$

$$\alpha_{ijk} = \cos^{-1} \frac{(x_i - x_j)(x_k - x_j) + (y_i - y_j)(y_k - y_j) + (z_i - z_j)(z_k - z_j)}{r_{ij} r_{ik}} \quad (10)$$

and the standard deviations through error propagation are given as [Uotila, 1967]

$$\sigma_{r_{ij}} = G \Sigma_{X_{ij}} G'$$

$$\sigma_{\alpha_{ijk}} = H \Sigma_{X_{ijk}} H' \quad (11)$$

where

$$\Sigma_{X_{ij}} = \begin{bmatrix} \Sigma X_i & \Sigma X_i X_j \\ & \Sigma X_j \end{bmatrix}_{6 \times 6}$$

$$\Sigma_{X_{ijk}} = \begin{bmatrix} \Sigma X_i & \Sigma X_i X_j & \Sigma X_i X_k \\ & \Sigma X_j & \Sigma X_j X_k \\ & & \Sigma X_k \end{bmatrix}_{9 \times 9}$$

$$G = \left[\frac{\partial r_{ij}}{\partial x_i} \frac{\partial r_{ij}}{\partial y_i} \frac{\partial r_{ij}}{\partial z_i} \frac{\partial r_{ij}}{\partial x_j} \frac{\partial r_{ij}}{\partial y_j} \frac{\partial r_{ij}}{\partial z_j} \right]$$

$$H = \left[\frac{\partial \alpha_{ijk}}{\partial x_i} \frac{\partial \alpha_{ijk}}{\partial y_i} \frac{\partial \alpha_{ijk}}{\partial z_i} \frac{\partial \alpha_{ijk}}{\partial x_j} \frac{\partial \alpha_{ijk}}{\partial y_j} \frac{\partial \alpha_{ijk}}{\partial z_j} \frac{\partial \alpha_{ijk}}{\partial x_k} \frac{\partial \alpha_{ijk}}{\partial y_k} \frac{\partial \alpha_{ijk}}{\partial z_k} \right]$$

Here, the typical partial derivatives are given as

$$\frac{\partial r_{ij}}{\partial x_i} = (x_i - x_j)/r_{ij}$$

$$\frac{\partial \alpha_{ijk}}{\partial x_i} = \frac{\sin \alpha_{ijk}}{r_{ij}^2 r_{ik}} [r_{ij}(x_k - x_j) - \cos \alpha_{ijk} r_{jk} (x_i - x_j)]$$

$$\frac{\partial \alpha_{ijk}}{\partial x_j} = \frac{\sin \alpha_{ijk}}{r_{ij}^2 \, r_{jk}^2} [r_{ij} r_{jk} (2x_j - x_i - x_k) + \cos \alpha_{ijk} \{r_{jk}^2 (x_i - x_j) + r_{ij}^2 (x_k - x_j)\}]$$

2.1.2 Short Arc Mode

2.1.2.1 General Comments

As mentioned earlier the dynamic methods in satellite goedesy are generally recognized as being either long arc or short arc. To obtain the necessary accuracy, the long arc method characteristically must employ such a complex mathematical model that is not available at present. However, the requirements in short arc mode are less stringent as the arc described is short and many approximations can be introduced without jeopardizing the accuracy. For the range observations in short arc mode, each participating station (P_i) observes the distances ($P_i Q_j$, $j = 1, 2, 3 \ldots$) to the satellite positions (Q_j) along an arc (Figure 2.1-9).

2.1.2.2 Equations of Motion

The motion of a satellite through space can be described by a set of three second-order differential equations, solution of which contains six arbitrary constants of integration. These six constants may take different forms depending on the variables in terms of which these differential equations are solved.

The solution to this set of differential equations may be written as

$$X_{(t)} = \int_{t_0}^{t} (t - \tau) F(\tau) d\tau + (t - t_0) \dot{x}(t_0) + x(t_0) \qquad (12)$$

where the constants of integration are the position and velocity vectors $x(t_0)$, $\dot{x}(t_0)$ at epoch time t_0 and $F(\tau)$ describes the force function at

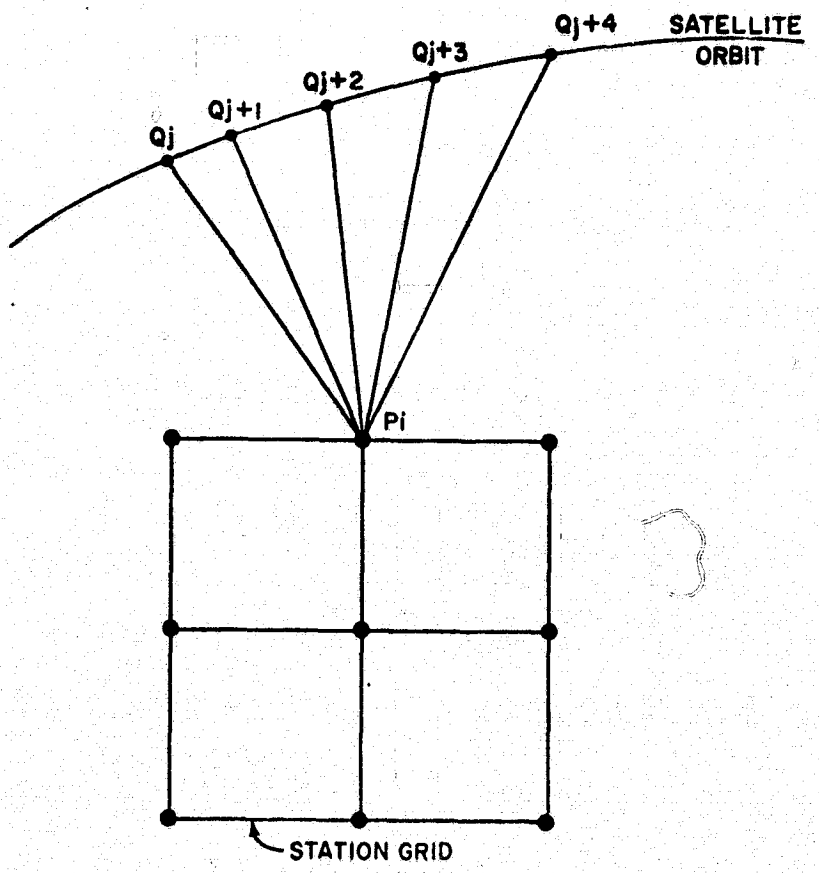

Fig. 2.1-9

any time τ during the flight.

The complexity of force function F determines the ease by which the integration may be carried out. Different methods have been suggested and employed for the solution of equation (12) using numerical integration, recurrent power series, polynomial fitting, analytical, hybrid, variation of elements, etc. [Hartwell, 1968; Hartwell and Lewis, 1967; Brown and Trotter, 1969; Gaposchkin, 1973; Anderle, 1974].

The important factors that effect the modeling of the motion and the subsequent solutions are as follows:

(a) force modeling both for gravitational and nongravitational forces

(b) truncation or approximation errors in the force function

(c) errors in the parameters of the model included in the force function

(d) errors of integration for equations of motion

(e) errors due to use of rotating coordinate system

If x_i, y_i, z_i, $\dot{x}_i$, $\dot{y}_i$, $\dot{z}_i$ denote the geocentric inertial state vector at any arbitrary time t_i, relative to an adopted epoch $t_0 = 0$, the power series solution of the equations of motion can be represented as [Brown and Trotter, 1969]:

$$\begin{bmatrix} x & \dot{x} \\ y & \dot{y} \\ z & \dot{z} \end{bmatrix} = \begin{bmatrix} a_0 & a_1 & a_2 & \cdots & a_n \\ b_0 & b_1 & b_2 & \cdots & b_n \\ c_0 & c_1 & c_2 & \cdots & c_n \end{bmatrix} \begin{bmatrix} 1 & 0 \\ t_i & 1 \\ t_i^2 & 2t_i \\ \vdots & \vdots \\ t_i^n & nt_i^{n-1} \end{bmatrix} \tag{13}$$

in which all the coefficients are functions of the six initial state vectors x_0, y_0, z_0, $\dot{x}_0$, $\dot{y}_0$, $\dot{z}_0$ at $t_0 = 0$ and of the gravitational coefficients alone. The series is truncated automatically when a prespecified tolerance is satisfied for the maximum value of t_i to be exercised. If the epoch t_0 is taken near mid-arc, the radius of convergence of each expansion in equation (13) is sufficiently great to accommodate as long as one-third of a revolution for nearly circular orbits.

The orbit generated by equation (13) can be referred to an earth-fixed framework by the transformation

$$\begin{bmatrix} X \\ Y \\ Z \\ \dot{X} \\ \dot{Y} \\ \dot{Z} \end{bmatrix} = \begin{bmatrix} R & 0 \\ \dot{R} & R \end{bmatrix} \begin{bmatrix} x \\ y \\ z \\ \dot{x} \\ \dot{y} \\ \dot{z} \end{bmatrix} \tag{14}$$

in which

$$R = \begin{bmatrix} \cos \omega t & \sin \omega t & 0 \\ -\sin \omega t & \cos \omega t & 0 \\ 0 & 0 & 1 \end{bmatrix} \tag{15}$$

and

$$\dot{R} = \omega \begin{bmatrix} -\sin \omega t & \cos \omega t & 0 \\ -\cos \omega t & -\cos \omega t & 0 \\ 0 & 0 & 0 \end{bmatrix} \tag{16}$$

This body-fixed orbit is then used to generate ranges corresponding to the observations and to form the discrepancy vector

$$\varepsilon = r_{ij} \text{ (computed)} - r_{ij} \text{ (observed)}. \tag{17}$$

A least squares adjustment from the discrepancy vector ε gives a body-fixed state vector at t_0 which when transformed to an inertial coordinate system can be used again in equation (13) to iterate.

2.1.2.3 Constraint Requirements

An inherent limitation of the short arc mode is that it falls short of uniquely defining the orbit around the earth and thereby locking it dynamically. The system consisting of ranges only will be solvable when sufficient constraints for the origin and orientation of the coordinate system in which the motion is described are applied.

The above requirement necessitates the inclusion of three distant fundamental stations in the system of whose six coordinates must be constrained to obtain stability of solutions. At least two of these fundamental stations must observe any given pass. If directional constraints are separately included, then constraining the three coordinates of any station will provide satisfactory solutions.

3. DATA GENERATION

A number of simulated experiments were designed to meet the different analysis approaches discussed in the previous chapter. These experiments required an extensive planning and care to select, set up and generate various satellite orbits and ranges. Details of generated orbits and ranges, different station configuration considered, and associated precision and accuracy of generated ranges are presented below.

3.1 Orbit Generation

Since the satellite orbit provides the connecting link in relating grid station positions to each other and their relative recovery, the basic tenet to suppress all possible resonances with the geopotential was to avoid orbital altitudes that will have periods commensurate with the earth's rotation. Knowing that the period of a satellite is given by the relation (assuming circular orbits)

$$T = 2\pi\sqrt{\frac{(a_e + H)^3}{GM}} \tag{1}$$

where

a_e = semi-major axis of the earth (6378 km)

H = altitude of the satellite

GM = gravitational constant x earth's mass (398 603 km^3/sec^2).

Thus, to avoid resonance

$$\frac{24^h}{T} \neq m,\ m + \frac{1}{2},\ m + \frac{1}{3},\ \ldots \tag{2}$$

where for a polar orbit the effect of regression of the ascending node for satellite orbit can also be omitted as first approximation. Combining

equations (1) and (2):

$$\frac{24^h\sqrt{GM}}{2\pi(a_e + H)^{\frac{3}{2}}} \neq m,\ m + \frac{1}{2}\ \ldots \tag{3}$$

Using the above equation, the following table gives the "critical" altitudes which are complemental to resonance m, $m + \frac{1}{2}$, ...

m	$m + \frac{1}{2}$	H (km)
	16.5	139.5
16		274.6
	15.5	416.9
15		567.0
	14.5	725.8
14		893.9
	13.5	1072.4
13		1262.2

Based on the above consideration, three orbital heights 392 km ($T = 92^m23^s.6$), 657 km ($T = 97^m52^s.3$) and 1007 km ($T = 105^m15^s.9$) were selected for experimentation. These orbits were then designated as lower (L), middle (M), and upper (U) in this report. In addition, another special case of "low-low" (LL) orbit was also considered to simulate an airplane flying at 9 km altitude. Figure 3.1-1 and Table 3.1-1 give the general coverage and distribution of observations in each of the four cases.

To simulate measurement systems either consisting of more than one satellite or using only one satellite but with highly eccentric orbit; different combinations of orbits were used in the solutions. The L + M combination then may represent an orbit with an eccentricity of about

$$e = \frac{\sqrt{(6378 + 657)^2 - (6378 + 392)^2}}{6378 + 657} = 0.27$$

and the L + U combination may represent an orbit with an eccentricity of about

$$e = \frac{\sqrt{(6378 + 1007)^2 - (6378 + 392)^2}}{6378 + 1007} = 0.40$$

In the geometric mode the following combinations of airplane and satellite were also considered: LL + L and LL + U.

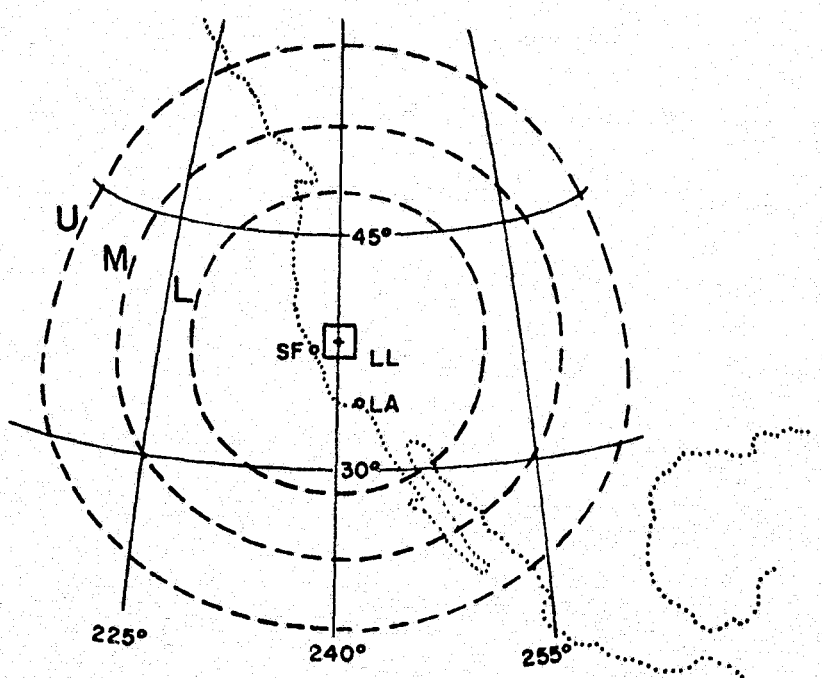

Fig. 3.1-1

Table 3.1-1

General Coverage Information for Different Orbits

Height of Orbit	Coverage* $\Delta\phi$	$\Delta\lambda$	Interval betw. Events to Obtain 5000 Events	Average Length of a Pass	No. of Req'd Passes	No. of Passes Per Day	Total Days Req'd
LL= 9 km	1°0	0°8	0.05 sec	10 sec	250	-	-
L= 392 km	19°0	24°0	1.0 sec	4 min	21	2	10 1/2
M= 657 km	27°8	35°2	1.0 sec	6 min	14	3	5
U=1007 km	37°0	46°8	1.0 sec	9 min	10	4	2 1/2

*Ideal weather conditions.

To obtain the most accurate satellite orbits and an extremely dense distribution of satellite points observable over a selected area, and distributed over a time frame of three to five days, the orbit generation was carried in the following two steps:

A. Long Arcs

In view of the stringent requirement of long arc (section 2.1.2.1) and the nonvisibility of most of the orbit over the specified small area, long arcs over 126 hours were used only to select satellite positions in passes where the satellite becomes visible for the first time from the grid stations. This requirement allowed the generation of the long arc with relaxed specifications and sparse density. Except for the orbital height variations, the other parameters were kept common in different cases as follows:

Inclination 90°

Eccentricity 0.001

Observational time span September 24, 1973 ($0^h.0$) to September 29, 1973 ($6^h.0$)

All the arcs were generated in True of Date (TOD) systems.

The computer program Goddard Trajectory Determining System (GTDS) was used in generation of long arcs [COSMIC, 1974; Wagner and Valez, 1972].

B. Short Arcs

From the long arcs in the L, M, and U orbital case, the portions of arcs were sorted out when the satellite in each case was over the specified area under consideration. The "starting" satellite position coordinates for each pass and for each orbital height were then used as input into GTDS program to generate short arcs to the position where the satellite would become nonvisible from the grid stations.

In generating these short arcs all possible refinements, e.g., inclusion of the latest geopotential model GEM 6, the latest solar radiation and air drag effects, of luni-solar perturbations, etc., as available in GTDS were utilized to simulate the orbits as near to reality as possible. The integration stepsize was also reduced to 10.0 s in place of default value of 24.0 s used in GTDS to increase the accuracy of the integrated orbits. All short arcs were generated in a body-fixed coordinate system.

Details on the number of short arcs and the density of satellite points generated for various orbital heights are given in Table 3.1.2.

The coverage pattern for h = 392 km is shown in Figure 3.1-2 with central station #5 in the center. The solid and broken lines show passes from south to north and vice versa, respectively. In about two days the satellite on pass #32 returns behind pass #1 (with a lag of about 3°) , and the cycle would repeat. In the cases of the M and U orbits, the passes trace back with 1° lag in about 3 days, and with 2°.5 lag in about 2 days, respectively.

Table 3.1-2

Generation Details for Short Arcs and Satellite Positions

Satellite Height (km)	Number of Short Arcs	Average Length of Each Arc (in time)	Density of Satellite Positions per Arc/s
9	30	10 s	20
392	35	8 m	10
	26	8 m	1
657	22	10 m	10
	31	10 m	1
1007	30	12 m	10
	30	12 m	1

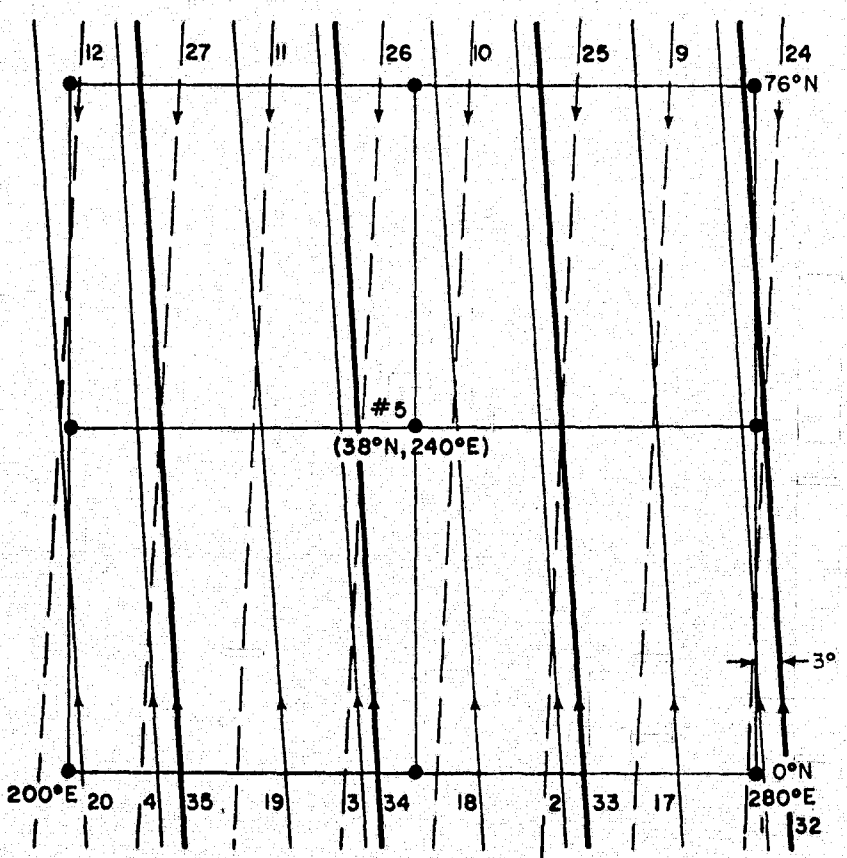

Fig. 3.1-2

For the airplane (LL), the coverage is more flexible as flight plans can be modified both in time and spacing.

3.2 Station Configuration

To keep the area near the San Andreas Fault, a grid configuration of 9 ground stations with the central station at ϕ = 38°N and λ = 240°E was selected. The remaining eight stations were placed at 5' separations, both in latitude and longitude from the central station (Figure 3.2-1).

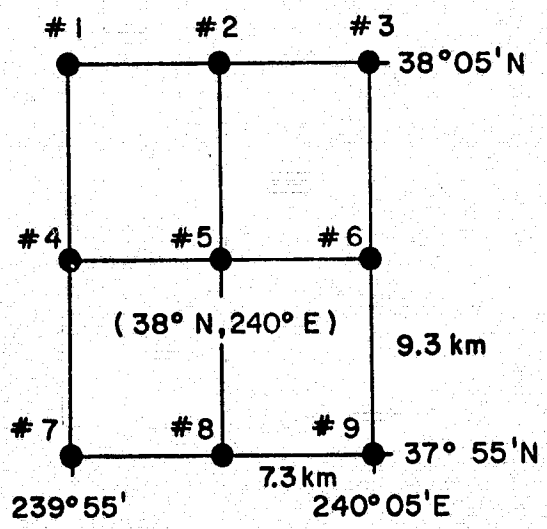

Fig. 3.2-1

3.2.1 Geometric Mode

With reference to earlier discussions (section 2.1.1.4) for studying the effect of near-critical configurations and improvement in the solution due to station separation in height away from the coplanar case, three different cases (A, B and C) were selected (Figure 3.2-2). The station height separations in the figure are not to scale. It is seen that the heights of stations #1, 5, 7, 2, 4, 6 and 8 in case B are one-tenth of case C, while stations #3 and 9 have zero height in all three cases.

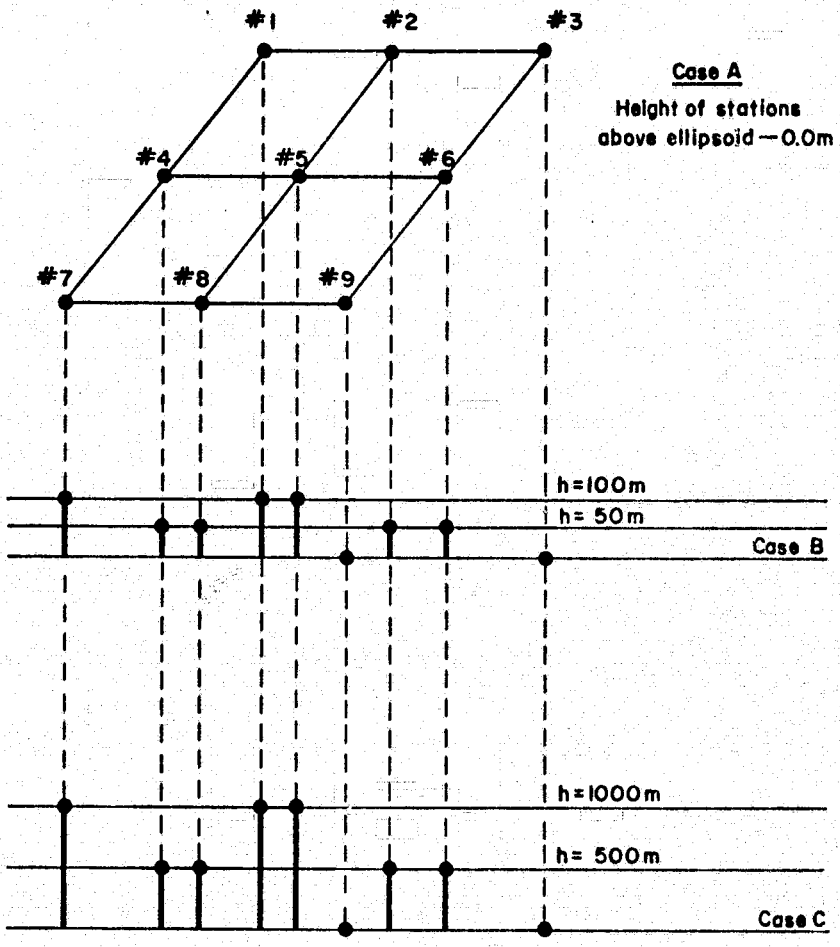

Fig. 3.2-2

3.2.2 Short Arc Mode

In the short arc mode, three distant stations were added (Figure 3.2-3) to define the origin and orientation of the system and to distinguish them from the nine "grid" stations; they are referred to as "fundamental" stations. These fundamental stations, in an actual experiment at a later stage, may be part of a large grid of stations or may be located at the Lageos station sites. In this simulation, they have been selected at the SAFE laser sites [Smith et al., 1974].

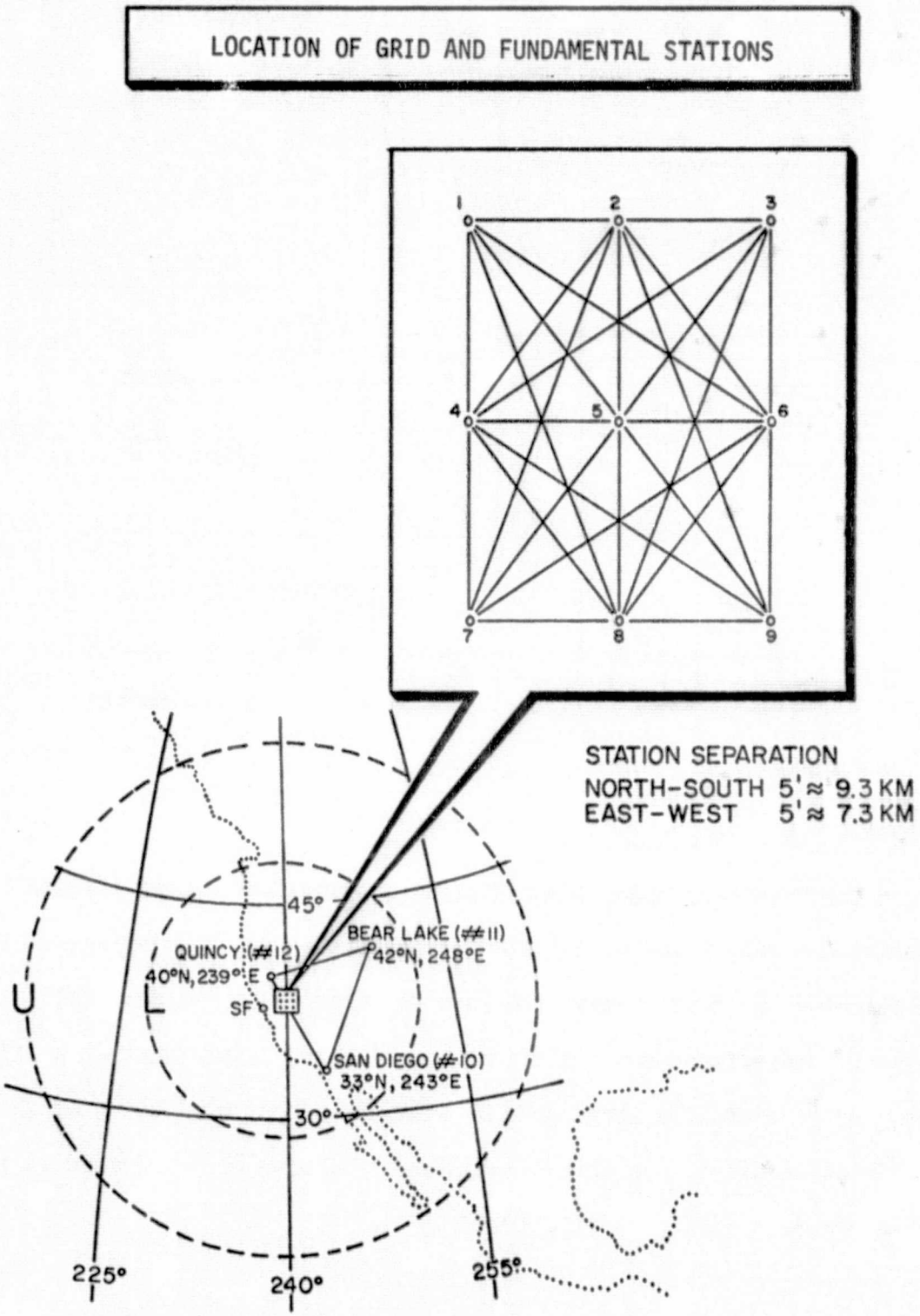
LOCATION OF GRID AND FUNDAMENTAL STATIONS
1
2
3
4
5
6
7
8
9
STATION SEPARATION
NORTH-SOUTH 5' ≈ 9.3 KM
EAST-WEST 5' ≈ 7.3 KM
45°
BEAR LAKE (#11)
42°N, 248°E
QUINCY (#12)
40°N, 239°E
SF
SAN DIEGO (#10)
33°N, 243°E
30°
225°
240°
255°

Fig. 3.2-3

3.3 Generation of Ranges

The Range Generation Program (RGP) and the short arcs (section 3.1.2) were used to generate ranges, both for the geometric (simultaneous) and the short arc (sequential and simultaneous) modes. Table 3.3-1 gives the details about the ranges generated.

Table 3.3-1

Generation of Ranges*

Satellite Height (km)	Geometric Mode			Short Arc Mode		
	No. of Passes	Case Type	Maximum Data Points Generated	No. of Passes	Case Type	Maximum Data Points Generated
9	30	A B C	3000 1500 1500	--	--	--
392	35	A B C	5000 5000 1000	26	A B C	5000 -- 500
657	22	A B C	500 5000 1000	--	--	--
1007	30	A B C	5000 5000 1000	30	A B C	5000 -- 500

*The main difference between the geometric and short arc modes is that the first requires ranges sorted event-wise and the second, station-wise along the passes.

During the range generation the density of orbit points was suitably altered between lower, middle and upper orbits to keep the number of ranges the same for each orbit with a cut-off maximum zenith distance of 75°.

3.4 Precision and Accuracy of Generated Ranges

The ranges which have been utilized in the present simulation were generated with a Gaussian noise (standard deviation) of 10 cm. However, in certain experimental cases "perfect" ranges were also used to investigate their effect on the system. It may be noted here that in the time scale of 3 to 5 years when the system under investigation may be operational, the overall precision (and accuracy) of laser ranging is expected to be significantly better than 10 cm [Weiffenbach, 1973]. The ranges used in this simulation were considered to be free of systematic errors.

4. SOLUTIONS PERFORMED

4.1 Geometric Mode Solutions

The software used to generate the solutions in the geometric mode is a Fortran program developed at The Ohio State University between 1966 and 1972 known as "The Ohio State University Geometric and Orbital (Adjustment) Program" (OSUGOP) [Reilly et al., 1972].

All solutions are summarized in Table 4.1-1. For each solution two numbers are listed. The upper number is the standard deviation in cm of the distance between the grid stations 1 and 2. The lower number is the same standard deviation divided by the distance itself in parts per million.

All the OSUGOP solutions were solved using inner constraints for the origin and orientation. Since this method yields nonestimable quantities (in this case coordinates), they were mapped into estimable quantities (chords between the stations and angles between the chords). A subroutine was added to OSUGOP which computes these angles and chords and their variances.

4.2 Short Arc Mode Solutions

The software used to generate the solutions in the geometric mode is a Fortran program developed by Duane Brown Associates between 1968 and 1973 known as "The Short Arc Geodetic Adjustment" (SAGA). A more detailed description of the capabilities of this program can be found in the two reports by Brown and Trotter [1969 and 1973]. The most important solutions are tabulated in Table 4.2-1. Due to the complexity of the problem, no numerical results are included. They may be found in the discussion in Section 5.

Table 4.1-1

$\sigma_{r_{12}}$ and $\sigma_{r_{12}}/r_{12}$

GEOMETRIC MODE SOLUTIONS									
No. of Observations per Station	Case	50	500				1000	2500	5000
No. of Grid Stations + No. of Fundamental Stations		9+0	9+0	9+1	9+2	9+3	9+0	9+0	9+0
Orbit: LL (9 km)	A	832.7 1139.0	277.0 378.0	-	-	-	158.6 217.0	114.5 156.7	-
	B	154.6 211.4	49.9 68.3	-	-	-	28.4 38.8	-	-
	C	18.0 24.6	6.0 8.2	-	-	-	3.4 4.7	-	-
L (392 km)	A	925.2 1265.5	289.7 396.2	-	-	-	204.8 280.1	129.5 177.2	91.2 124.7
	B	176.7 241.6	53.9 73.7	-	-	-	38.1 52.1	24.1 32.9	17.0 23.2
	C	19.9 27.1	5.9 8.1	-	-	-	4.2 5.7	-	-
M (657 km)	A	-	249.5 341.2	-	-	-	-	-	-
	B	142.6 195.1	43.0 58.9	-	-	-	30.0 41.1	19.1 26.1	13.4 18.3
	C	15.5 21.2	4.7 6.4	-	-	-	3.3 4.5	-	-
U (1007 km)	A	739.8 1011.9	238.2 325.7	2.9 4.0	2.3 3.2	1.2 1.7	168.6 230.6	106.1 145.2	74.7 102.2
	B	123.3 168.7	38.6 52.8	-	-	-	27.3 37.3	17.2 23.5	12.1 16.5
	C	13.5 18.5	4.1 5.6	3.2 4.4	3.4 4.6	1.3 1.7	2.9 4.0	-	-
LL+L	A	-	2.2 3.1	-	-	-	-	-	-
	B	-	-	-	-	-	-	-	-
	C	-	-	-	-	-	-	-	-
LL+U	A	-	2.2 3.0	-	-	-	-	-	-
	B	-	-	-	-	-	-	-	-
	C	-	-	-	-	-	-	-	-
L+M	A	-	128.1 175.3	-	-	-	-	-	-
	B	-	43.8 59.9	-	-	-	-	-	-
	C	-	5.0 6.9	-	-	-	-	-	-
L+M+U	A	-	109.3 149.4	-	-	-	-	-	-
	B	-	39.8 54.4	-	-	-	-	-	-
	C	-	4.6 6.2	-	-	-	-	-	-

Table 4.2-1

SHORT ARC MODE SOLUTIONS														
Case	No. of Observations per Station	250								500			750	1000
	No. of Grid Stations + No. of Fundamental Stations	9+3	6+3	4+3	9+2	7+2	4+2	3+2	9+1	9+3	6+3	7+2	9+3	9+3
A	Orbit: L	4*											x	
C														
A	U	2**	2**	x	x	x	x	x	x	x	x	x		x
C										x				
A	L+U									x				
C														

*Four solutions using the following gravity models: SAGA (8x8). GEM 6 (J_0 only), GEM 6 (J_0, J_2 only) and GEM 6 (8x8 only).

**Two solutions both with simultaneous and sequential observations.

5. RESULTS

The initial analysis for the geometric mode differed from the analysis for the short arc mode in a number of aspects which are described below.

Geometric Mode. Due to the simplicity of the model only a variance analysis was performed, and the standard deviations of the recovered distances between the grid stations were investigated. A linear dependency between the standard deviation $\sigma_{r_{ij}}$ and the distance r_{ij} became clear as the following examples show (Figures 5-1, 5-2, 5-3, and Table 5-1). In these figures $\sigma_{r_{ij}}$ is plotted against r_{ij} for 500 observations per station. Three graphs for the height differences 0 m, 100 m and 1000 m (cases A, B, and C) show that the linear dependency increases with the height difference between the grid stations. Only the distances between grid point 1 and all the other grid stations were considered (r_{ij}, j=2, ... 9) since this set of 8 distances turned out to be a representative set of all the possible 36 distances between the 9 grid stations.

In Figures 5-1 through 5-6, the interruption in the linear trend occurs for the distance r_{13} ($\approx$ 15 km) where the distance under consideration lies more or less perpendicular to the satellite orbit. It may be quite possible that in case of a nonpolar orbit this interruption may disappear.

An alternative representation was also chosen where the variations of the relative standard deviations $\sigma_{r_{ij}}/r_{ij}$ with the distances r_{ij} were investigated. The units for the relative standard deviation are expressed in parts per million. The same three graphs are plotted as before except the ordinates are $\sigma_{r_{ij}}/r_{ij}$ instead of $\sigma_{r_{ij}}$ (Figures 5-4, 5-5, 5-6,and Table 5-1).

Table 5-1

$\sigma_{r_{ij}}$ (cm), Upper Number, and $\sigma_{r_{ij}}/r_{ij}$ (p.p.m.), Lower Number, As a Function of Orbital Height and Station Height Difference (500 Observations per Station)

Case	i - j	1 - 2	1 - 3	1 - 4	1 - 5	1 - 6	1 - 7	1 - 8	1 - 9
A	$r_{ij_{km}}$	7.311	14.622	9.250	11.793	17.309	18.499	19.895	23.591
	LL	277.0 378.8	554.3 379.1	296.0 320.0	330.4 280.1	541.2 312.7	594.1 321.1	592.6 297.9	663.5 281.3
	L	289.7 396.2	579.5 396.3	206.4 223.2	258.5 219.2	517.7 299.1	412.8 223.2	413.2 207.7	517.6 219.4
	M	249.5 341.2	498.9 341.2	208.4 225.4	258.5 219.2	468.1 270.4	416.8 225.3	427.2 214.8	517.2 219.2
	U	238.2 325.7	476.2 325.7	237.2 256.5	275.7 233.7	460.6 266.1	474.3 256.4	479.5 241.0	551.4 233.6
	LL+L	2.2 3.1	4.1 2.8	1.9 2.0	2.2 1.8	3.8 2.2	3.3 1.8	3.3 1.7	3.9 1.7
	LL+U	2.2 3.0	3.8 2.6	1.8 2.0	2.1 1.8	3.5 2.0	3.1 1.7	3.1 1.6	3.7 1.6
	L+M	128.1 175.3	256.3 175.3	102.7 111.0	122.0 103.4	232.0 134.0	205.4 111.0	204.1 102.6	244.1 103.5
	L+M+U	109.3 149.4	218.5 149.4	88.4 95.6	105.8 89.7	199.2 115.1	176.7 95.5	176.6 88.8	211.7 89.7
B	$r_{ij_{km}}$	7.311	14.623	9.250	11.793	17.310	18.500	19.895	23.591
	LL	49.9 68.3	99.5 68.0	70.6 76.4	87.2 73.9	123.9 71.6	141.2 76.3	150.5 75.7	175.2 74.2
	L	53.9 73.7	107.8 73.7	43.6 47.0	57.2 48.5	103.4 59.7	87.3 47.2	91.5 46.0	114.4 48.5
	M	43.0 58.9	86.0 58.8	42.8 46.3	58.9 49.9	93.5 54.0	85.6 46.3	94.6 47.6	117.6 49.9
	U	38.6 52.8	77.1 52.7	47.1 50.9	59.3 50.2	87.5 50.6	94.3 51.0	100.4 50.5	118.4 50.2
	L+M	43.8 59.9	87.5 59.9	40.2 43.4	51.0 43.2	86.7 50.1	80.4 43.5	84.3 42.4	101.9 43.2
	L+M+U	39.8 54.4	79.5 54.4	40.3 43.6	49.0 41.6	80.0 46.2	80.6 43.6	83.5 42.0	98.0 41.5

Table 5-1 (cont'd)

Case	i - j	1 - 2	1 - 3	1 - 4	1 - 5	1 - 6	1 - 7	1 - 8	1 - 9
C	$r_{ij_{km}}$	7.329	14.658	9.264	11.795	17.319	18.502	19.903	23.614
	LL	6.0 8.2	11.4 7.8	8.8 9.5	10.4 8.8	14.6 8.4	16.8 9.1	17.9 9.7	20.6 8.7
	L	5.9 8.1	11.7 8.0	4.8 5.2	6.4 5.5	11.4 6.6	9.6 5.2	10.1 5.1	12.7 5.4
	M	4.7 6.4	9.2 6.3	4.7 5.1	6.6 5.6	10.2 5.9	9.5 5.1	10.4 5.2	12.8 5.4
	U	4.1 5.6	8.1 5.5	5.2 5.6	6.6 5.6	9.4 5.4	10.4 5.6	11.0 5.5	12.8 5.4
	L+M	5.0 6.9	9.9 6.8	4.7 5.1	6.3 5.3	10.3 6.0	9.4 5.1	10.1 5.1	12.4 5.2
	L+M+U	4.6 6.2	8.9 6.1	4.9 5.3	6.3 5.3	9.7 5.6	9.8 5.3	10.3 5.2	12.2 5.2

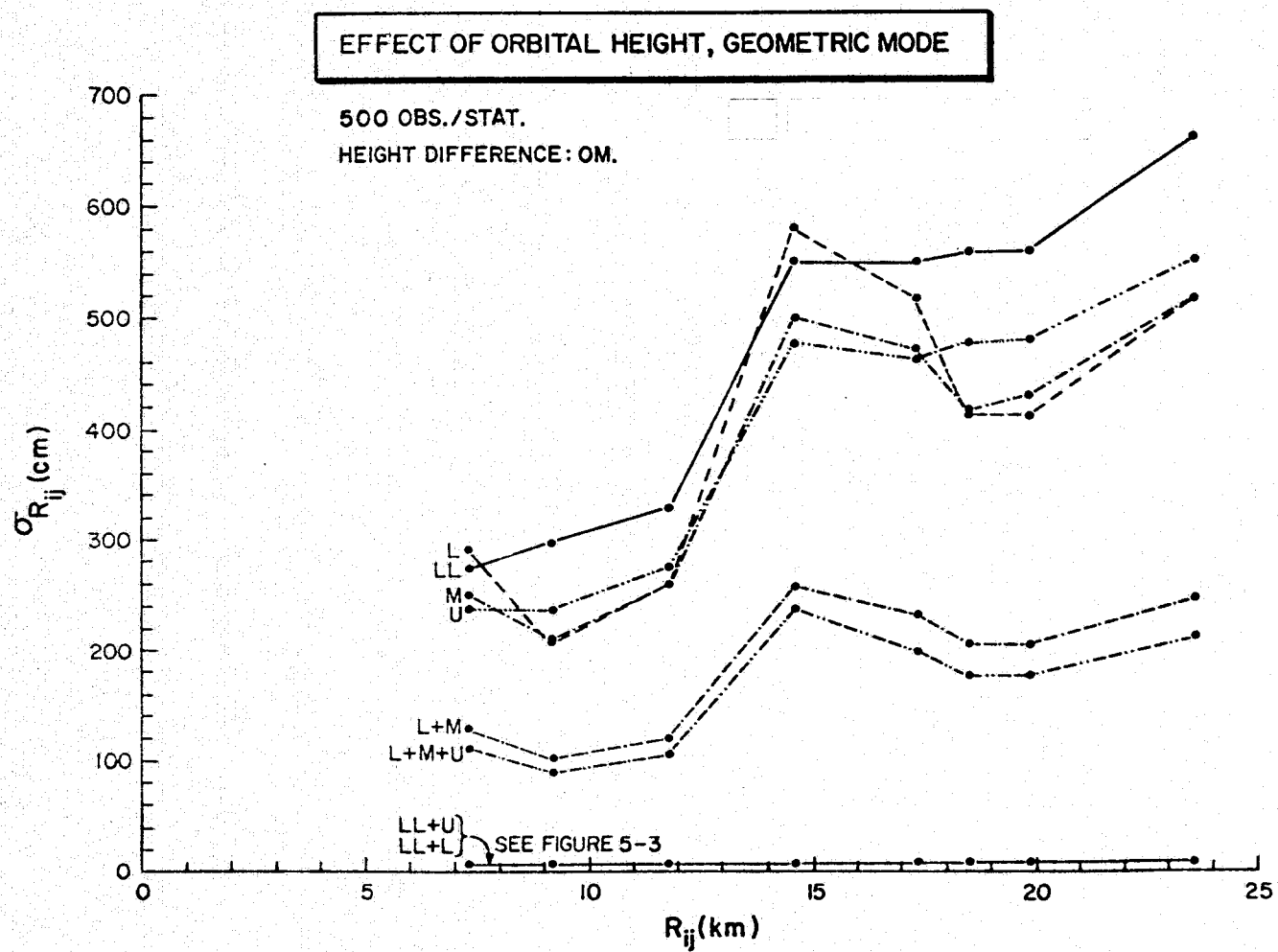
EFFECT OF ORBITAL HEIGHT, GEOMETRIC MODE
500 OBS./STAT.
HEIGHT DIFFERENCE: OM.
700
600
500
400
300
200
100
0
$\sigma_{R_{ij}}$ (cm)
0
5
10
15
20
25
R_{ij} (km)
L
LL
M
U
L+M
L+M+U
LL+U
LL+L
SEE FIGURE 5-3

Fig. 5-1

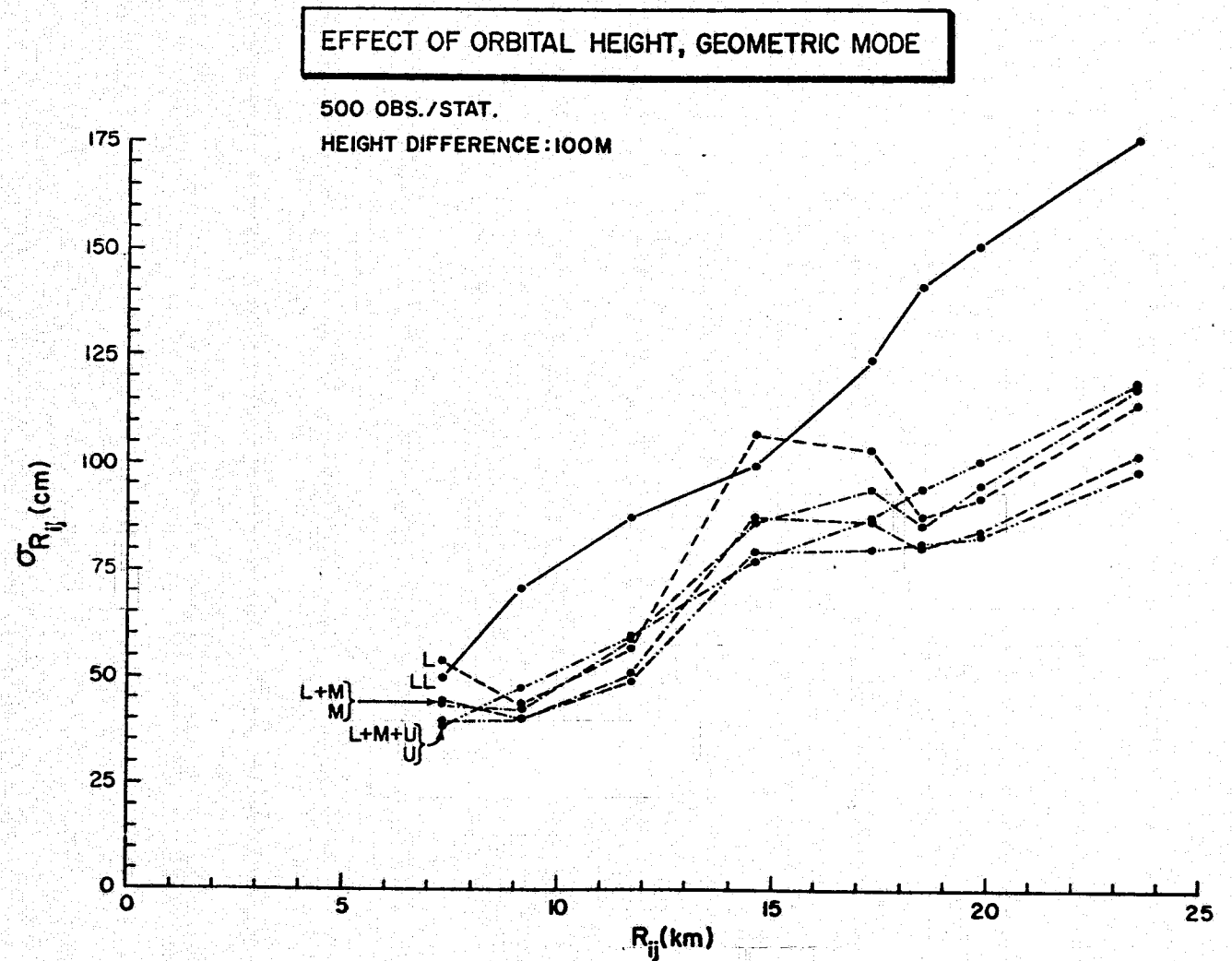
EFFECT OF ORBITAL HEIGHT, GEOMETRIC MODE
500 OBS./STAT.
HEIGHT DIFFERENCE: 100M
175
150
125
100
75
50
25
0
$\sigma_{R_{ij}}$ (cm)
0
5
10
15
20
25
R_{ij}(km)
L
LL
L+M
M
L+M+U
U

Fig. 5-2

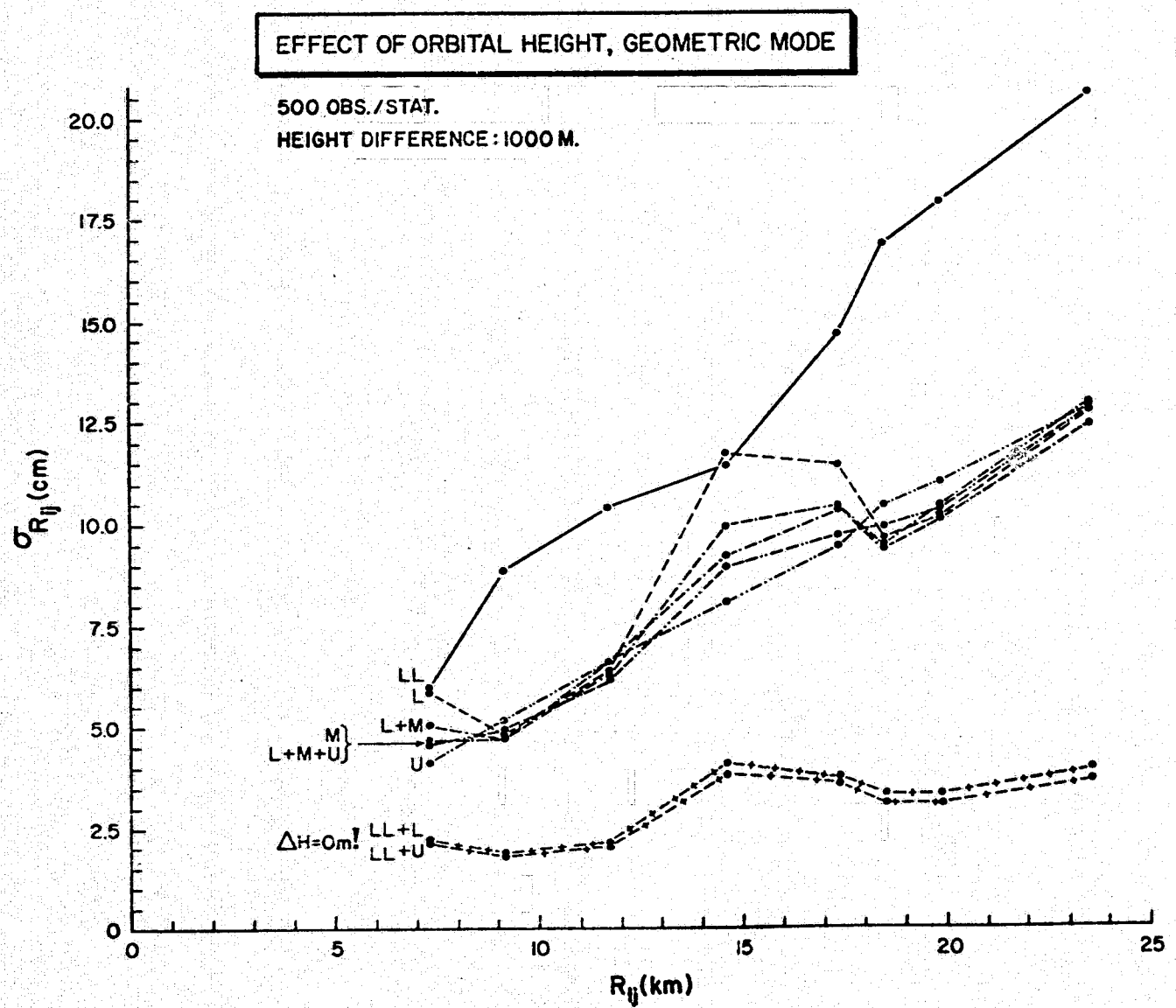
EFFECT OF ORBITAL HEIGHT, GEOMETRIC MODE
500 OBS./STAT.
HEIGHT DIFFERENCE: 1000 M.
20.0
17.5
15.0
12.5
10.0
7.5
5.0
2.5
0
$\sigma_{R_{ij}}$(cm)
LL
L
M
L+M+U
L+M
U
ΔH=0m!
LL+L
LL+U
0
5
10
15
20
25
R_{ij}(km)

Fig. 5-3

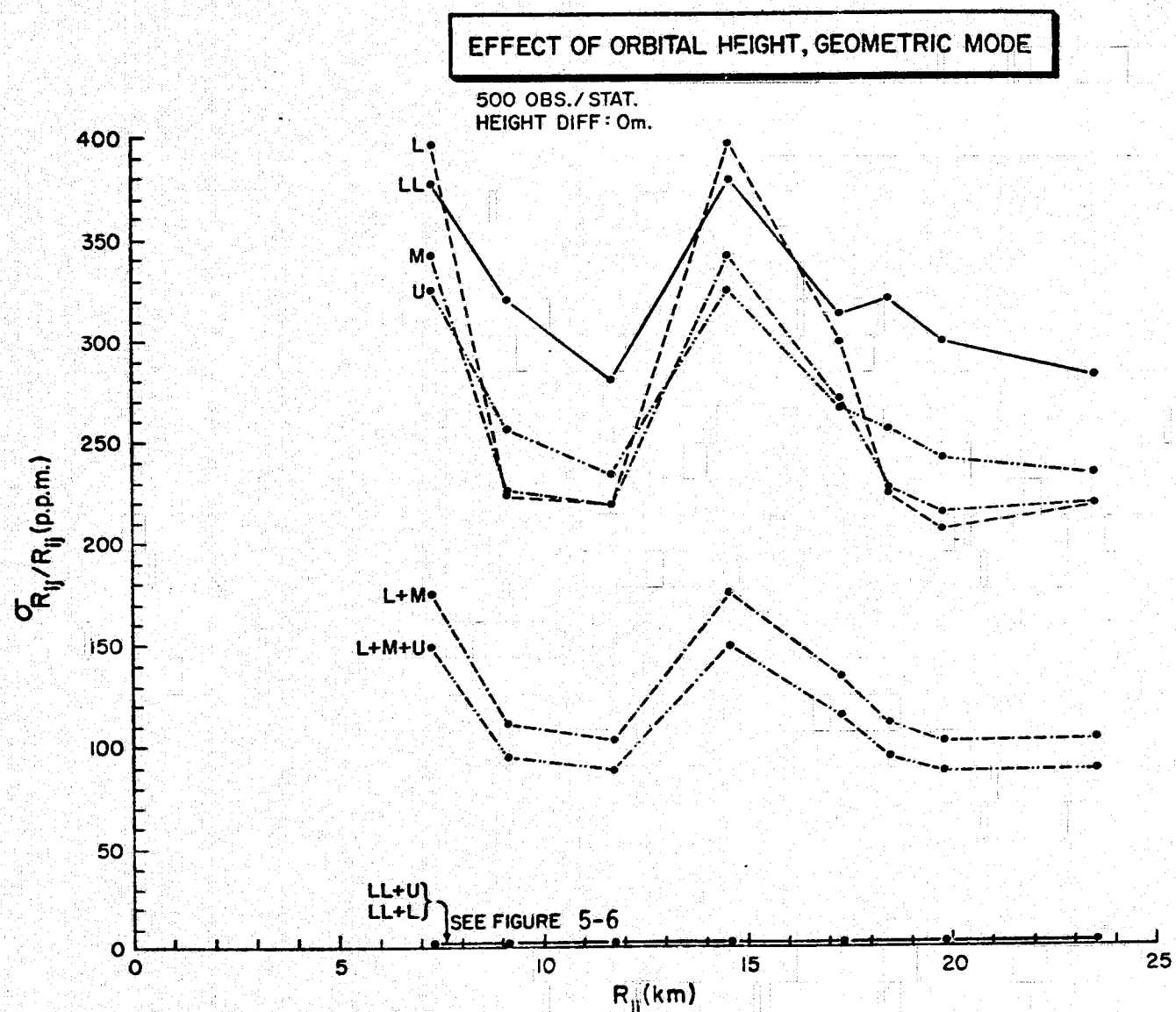
EFFECT OF ORBITAL HEIGHT, GEOMETRIC MODE
500 OBS./STAT.
HEIGHT DIFF: 0m.
L
LL
M
U
L+M
L+M+U
LL+U
LL+L
SEE FIGURE 5-6
400
350
300
250
200
150
100
50
0
0
5
10
15
20
25
$\sigma_{R_{ij}}/R_{ij}$ (p.p.m.)
R_{ij} (km)

Fig. 5-4

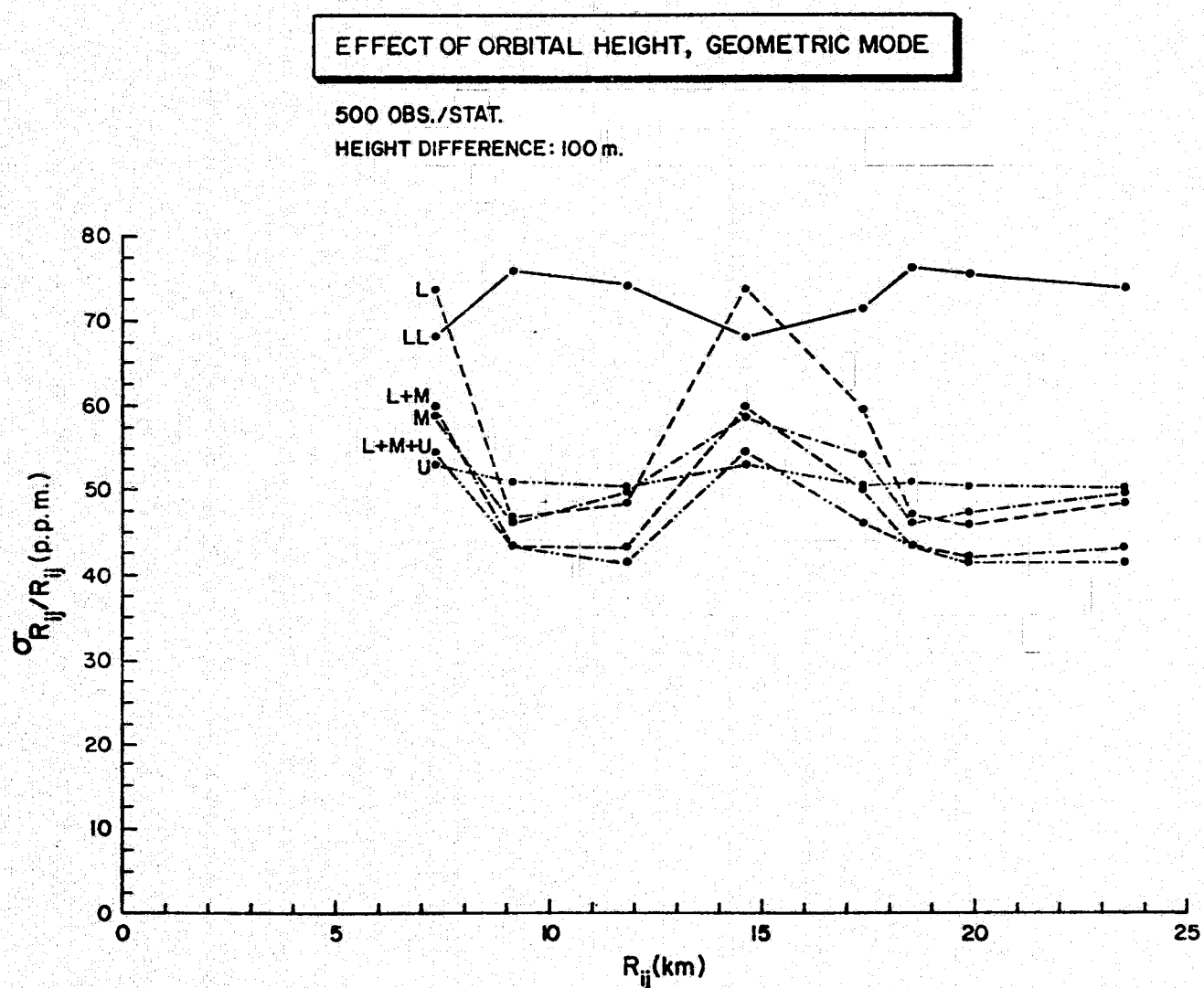
EFFECT OF ORBITAL HEIGHT, GEOMETRIC MODE
500 OBS./STAT.
HEIGHT DIFFERENCE: 100 m.
L
LL
L+M
M
L+M+U
U
$\sigma_{R_{ij}}/R_{ij}$ (p.p.m.)
R_{ij}(km)
0
10
20
30
40
50
60
70
80
0
5
10
15
20
25

Fig. 5-5

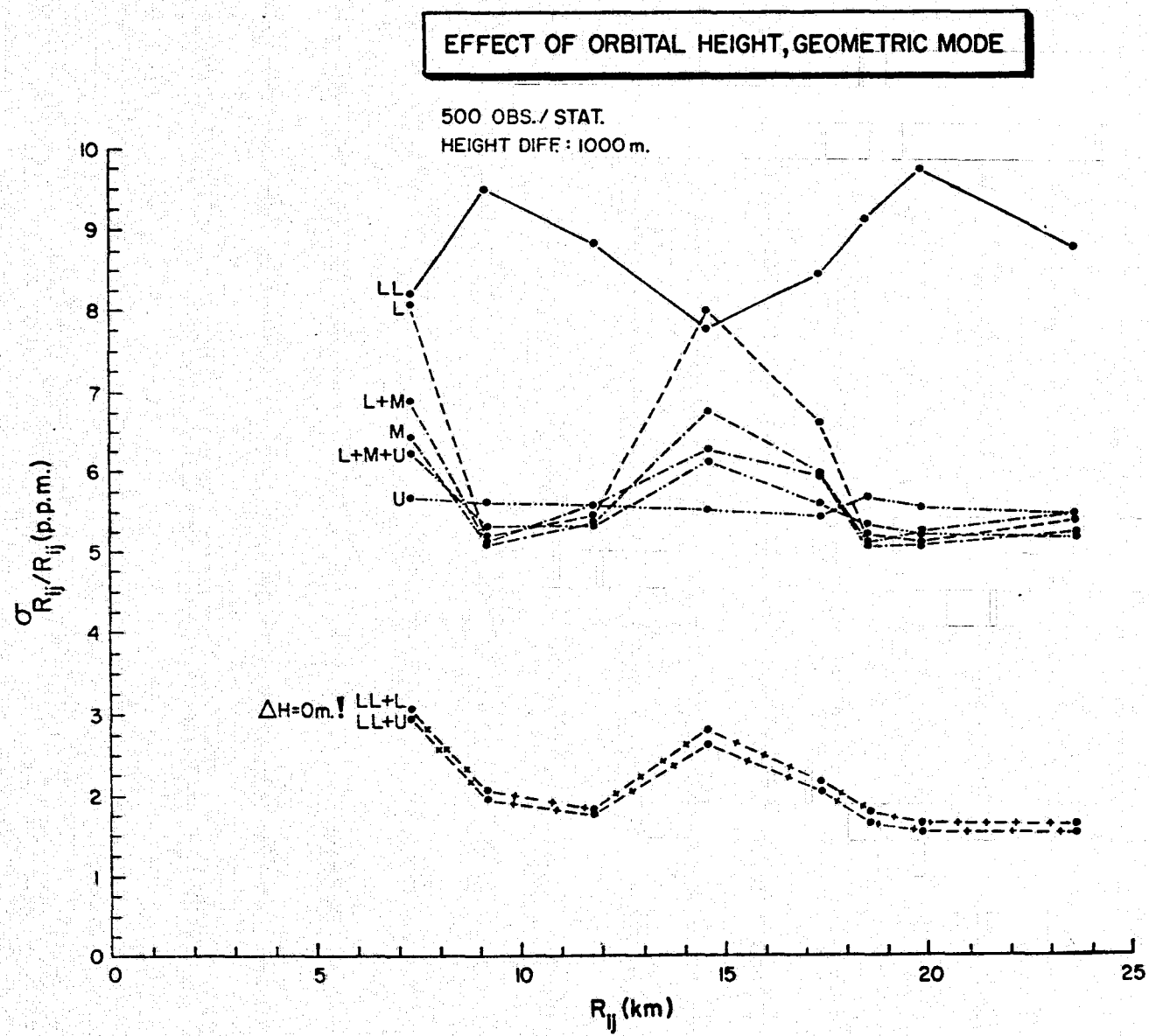
EFFECT OF ORBITAL HEIGHT, GEOMETRIC MODE
500 OBS./ STAT.
HEIGHT DIFF. : 1000 m.
LL
L
L+M
M
L+M+U
U
ΔH=0m.!
LL+L
LL+U
$\sigma_{R_{ij}}/R_{ij}$ (p.p.m.)
R_{ij} (km)
0
5
10
15
20
25
1
2
3
4
6
7
8
9
10

Fig. 5-6

A similar variance analysis was performed for the angles between the chords (Figure 5-7 and Table 5-2). A representative set of angles was chosen: the horizontal angles α, e.g., ∢253 and ∢256 (the behavior of these angles is very similar to the distances r_{ij}); the vertical angles β, e.g., ∢456 and ∢258 (the behavior of these angles is related to the strength of the network in the vertical direction, i.e., in height). See Table 5.2.

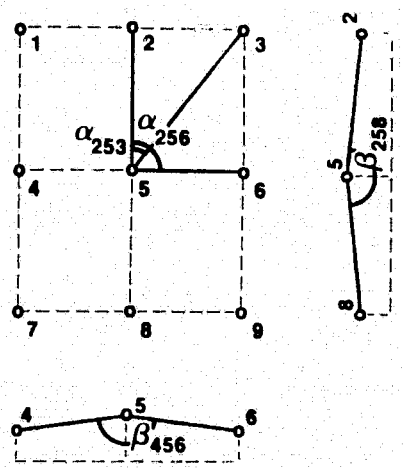

Fig. 5-7

Short arc mode. Instead of a variance analysis, a recovery analysis was performed for quantities least affected by the systematic modeling errors, namely, the distances between the grid stations. The representation in this case is in terms of residuals computed as the difference between the recovered distances and the true distance between the grid stations.

Geometric mode vs. short arc mode. In the final analysis which compares the geometric mode against the short arc mode, the common denominator of the analysis was the recovery of the distances between the grid stations.

Table 5-2

Standard Deviations of Recovered Angles in Radians x 10^{-6}
(500 Observations per Station)

		α		β	
Case	ijk	253	256	456	258
	α,β ijk	~45°	~90°	~180°	~180°
A	LL	314.12	395.88	424.13	558.29
	L	277.19	295.14	13.84	12.13
	M	258.29	319.33	7.81	7.87
	U	268.14	352.96	5.81	6.45
	LL+L	[illegible]04	2.46	3.40	2.96
	LL+U	1.98	2.44	3.23	2.71
	L+M	115.39	109.66	5.56	5.32
	L+M+U	96.87	91.71	4.49	4.19
	α,β ijk	~45°	~90°	~180°	~180°
B	LL	61.87	100.89	96.20	135.40
	L	51.89	63.30	6.62	4.70
	M	47.20	73.87	4.33	3.56
	U	47.24	77.47	4.07	3.49
	L+M	44.37	58.04	4.90	3.84
	L+M+U	41.70	55.68	4.41	3.59
	α,β ijk	~45°	~90°	~180°	~180°
C	LL	6.96	11.75	14.48	19.13
	L	5.65	6.96	4.48	3.21
	M	5.21	8.11	3.56	2.74
	U	5.10	8.32	3.56	2.84
	L+M	5.25	7.34	3.85	2.91
	L+M+U	5.08	7.49	3.67	2.85

The questions to which answers were sought through the analysis were the following: How is the recovery of distances affected by

(1) the altitude of the satellite

(2) the number of observations

(3) the number of stations and their distribution

(4) the coplanarity of the stations

(5) the mode of the observations

(6) the algorithm.

These considerations are elaborated on below for both modes of analysis.

5.1 Altitude of Satellites and Airplanes

5.1.1 Geometric Mode

Considering only the worst case whereby the stations are situated near a plane, it is obvious from Tables 4.1-1, 5-1 and Figure 5-1 that a single measurement system (i.e., one satellite at various altitudes or an airplane) cannot obtain an efficiency factor of 1. (The efficiency factor in this case is the ratio of the standard deviation of the recovered distance between two grid stations and the standard deviation of the range measurement σ_r = 10 cm).

It can be seen from Table 5-2 that the vertical control of the network (β angles) is much better determined than the horizontal control (by at least a factor of 20). Summarizing, except for the vertical control, single measurement systems are unable to recover relative station positions with an efficiency factor of 1.

An improvement, although not spectacular, is the combination of satellite orbits, i.e., lower and middle orbit combined or lower, middle and upper orbit combined.

The best measurement system seems to be the combination of the airplane and the satellite. From Table 4.1-1 and Figures 5-1 and 5-4, it can be seen that the efficiency factor exceeds 1 impressively (E.F.≈ 1/5); thus fewer than 500 observations (~50 - 100) should be sufficient.

The tables and figures mentioned in this section are summarized in Tables 5.1-1 and 5.1-2.

Table 5.1-1

500 Observations per Station, Case A (ΔH = 0 m)

r_{12} = 7.311107 km	$\sigma_{r_{12}}$ cm	$\sigma_{r_{12}}/r_{12}$ ppm	$\sigma_{\alpha_{253}}$ x 10^{-6} rad	$\sigma_{\beta_{456}}$ x 10^{-6} rad
LL	277	378.8	314.12	424.13
L	290	396.2	277.19	13.84
M	250	341.2	258.29	7.81
U	238	325.7	268.14	5.81
LL+L	2	3.1	2.04	3.40
LL+U	2	3.0	1.98	3.23
L+M	128	175.3	115.39	5.56
L+M+U	109	149.4	96.87	4.49

Table 5.1-2

Percentage of Residuals (Absolute)

Residuals	0 - 1 cm	1 - 2 cm	2 - 3 cm	3 - 4 cm	>4 cm	Max Res
LL+L	69	28	3	--	--	3 cm
LL+U	81	19	--	--	--	2 cm

The combination of an airplane and a satellite in a high orbit (1007 km) seems to be more favorable than the combination with a low satellite (392 km).

5.1.2 Short Arc Mode

In this mode only two orbital altitudes have been investigated, the lower and the upper orbits. As it may be seen from Table 5.1-3 and Figure 5.1-1, the upper orbit gives better recovery than the lower orbit, probably due to possible modeling deficiency of the force field in which the satellite moves.

A clear scale-type effect is visible from the histograms in Figure 5.1-1 and from Figures 5.1-2 and 5.1-3. A shift to the negative side can be recognized. The reason for this effect is unexplained at the present time.

5.2 Number of Observations per Station

5.2.1 Geometric Mode

In the near critical configurations the number of observations played only the conventional role that when increasing the number of observations by a factor of n, the efficiency factor decreased by a factor of $\sqrt{n}$.

As an example (from Table 4.1-1), for 50 observations per station in the lower orbit, the efficiency factor was

$$E.F. = \frac{\sigma_{r_{12}}}{\sigma_r} = \frac{925}{10} = 92.5$$

while for 5000 events

$$E.F. = \frac{\sigma_{r_{12}}}{\sigma_r} = \frac{91}{10} = 9.1 \cong \frac{92.5}{\sqrt{\frac{5000}{50}}}$$

In the best measurement system (airplane + satellite), the efficiency factor was already 1/5 for 500 observations per station. Consequently, the number of observations per station should not have been a factor of

Table 5.1-3

Effect of Orbital Height

#	Orbit	Case	Fundamental Stations per Pass	Grid Stations per Pass	Days	Observations per Station				σ_r (cm)	Results	
						Passes	Minimum Events per Pass	Total Observations per Station	Total Observations		Residuals in cm	Spread cm
5	upper	A	3	9	3	9	8	239	2868	10	10 <Δx< 15 2 <Δy< 8 - 34 <Δz< - 29 - 7 <Δr< 2	5 6 5 9
8	lower	A	3	9	5	7	10	254	3048	10	39 <Δx< 51 81 <Δy< 99 -160 <Δz< -143 - 9 <Δr< 1	12 18 17 10
2	upper	A	3	9	3	9	15	483	5796	10	4 <Δx< 7 1 <Δy< 7 - 37 <Δz< - 31 - 6 <Δr< 0	3 6 6 6
13	lower	A	3	9	5	7	29	758	9096	10	36 <Δx< 51 79 <Δy< 98 -163 <Δz< -147 - 9 <Δr< 2	15 19 16 11

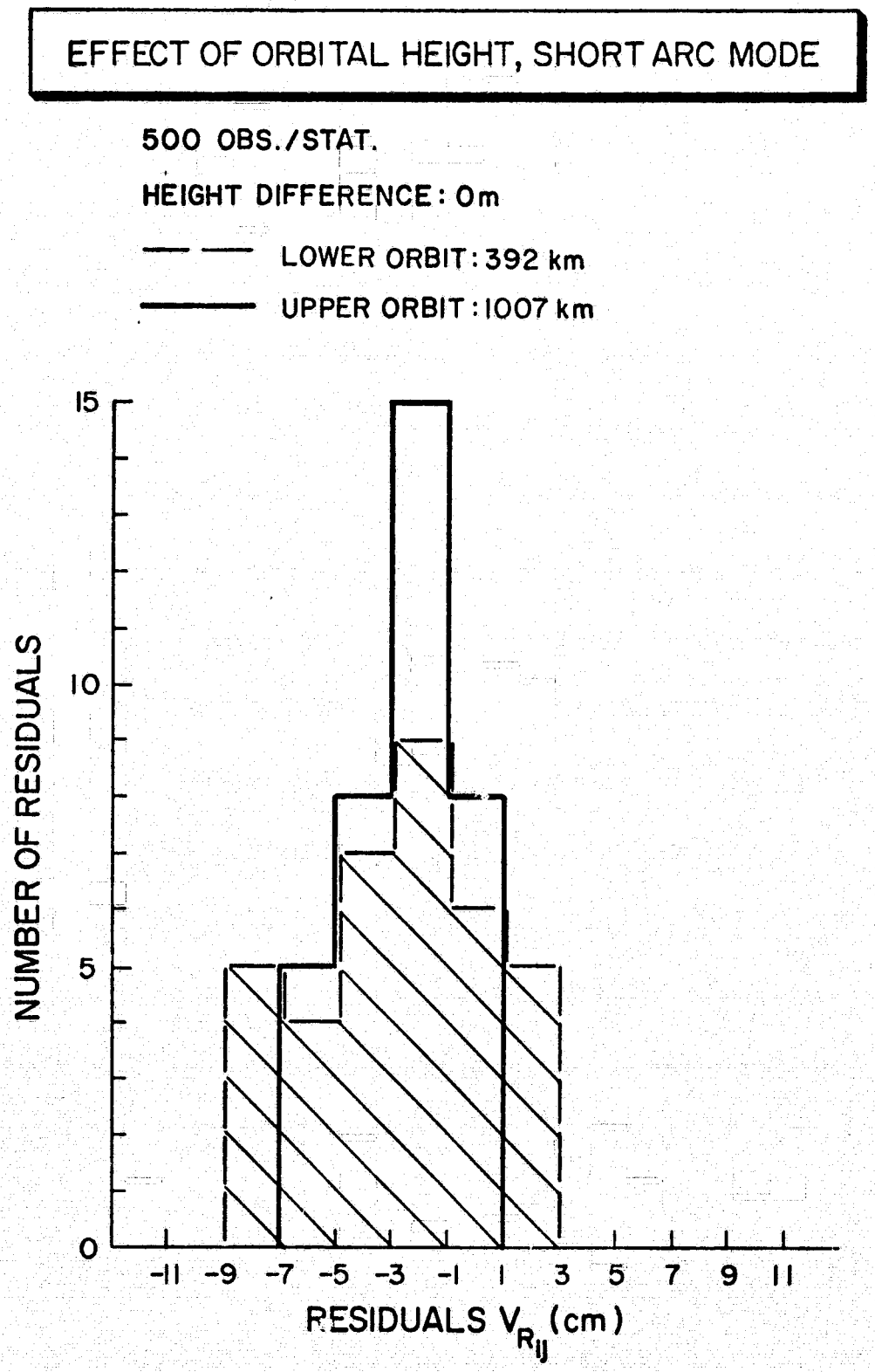
EFFECT OF ORBITAL HEIGHT, SHORT ARC MODE
500 OBS./STAT.
HEIGHT DIFFERENCE: 0m
LOWER ORBIT: 392 km
UPPER ORBIT: 1007 km
NUMBER OF RESIDUALS
15
10
5
0
-11 -9 -7 -5 -3 -1 1 3 5 7 9 11
RESIDUALS $V_{R_{ij}}$ (cm)

Fig. 5.1-1

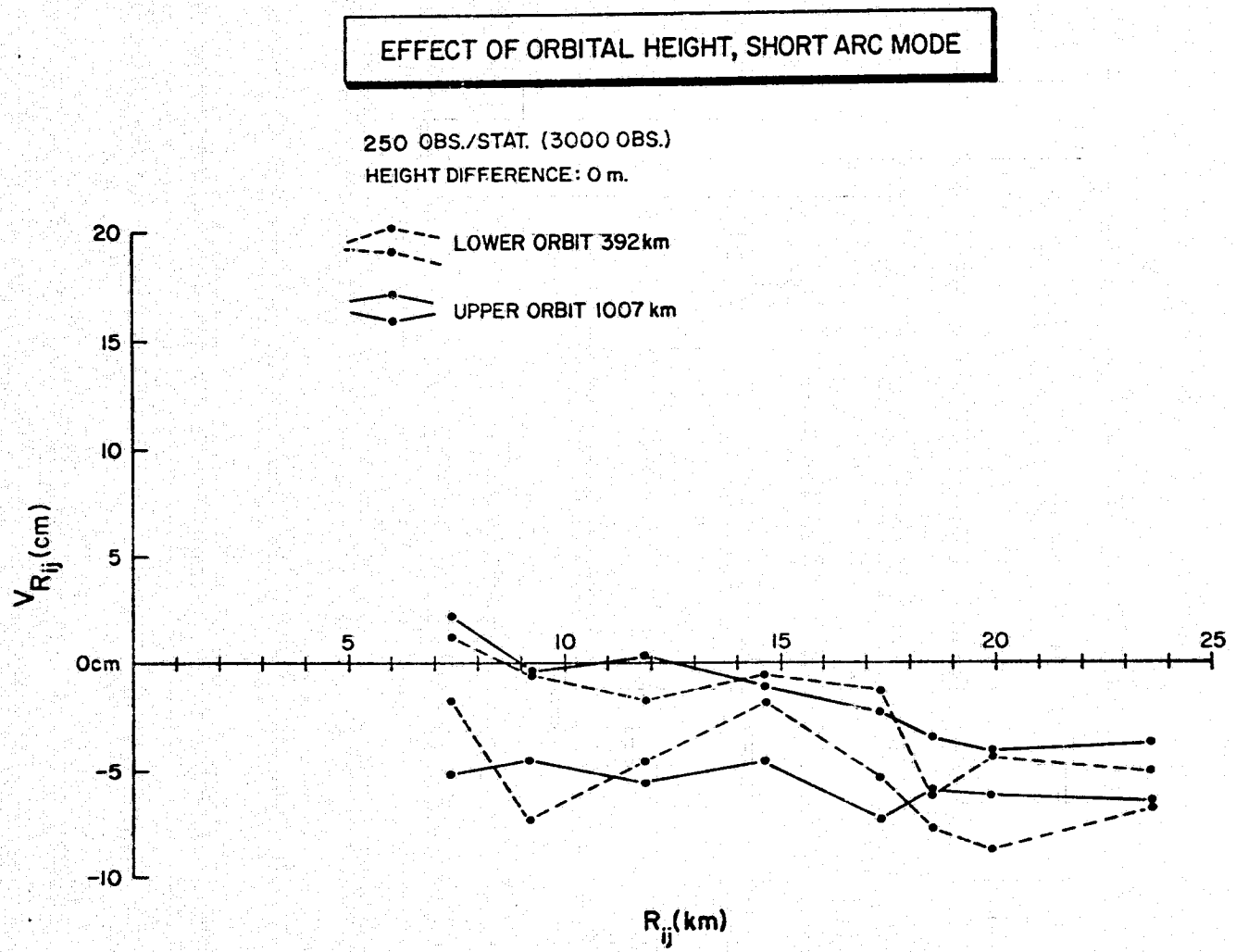
EFFECT OF ORBITAL HEIGHT, SHORT ARC MODE
250 OBS./STAT. (3000 OBS.)
HEIGHT DIFFERENCE: 0 m.
LOWER ORBIT 392km
UPPER ORBIT 1007 km
20
15
10
5
0cm
-5
-10
5
10
15
20
25
$V_{R_{ij}}$(cm)
R_{ij}(km)

Fig. 5.1-2

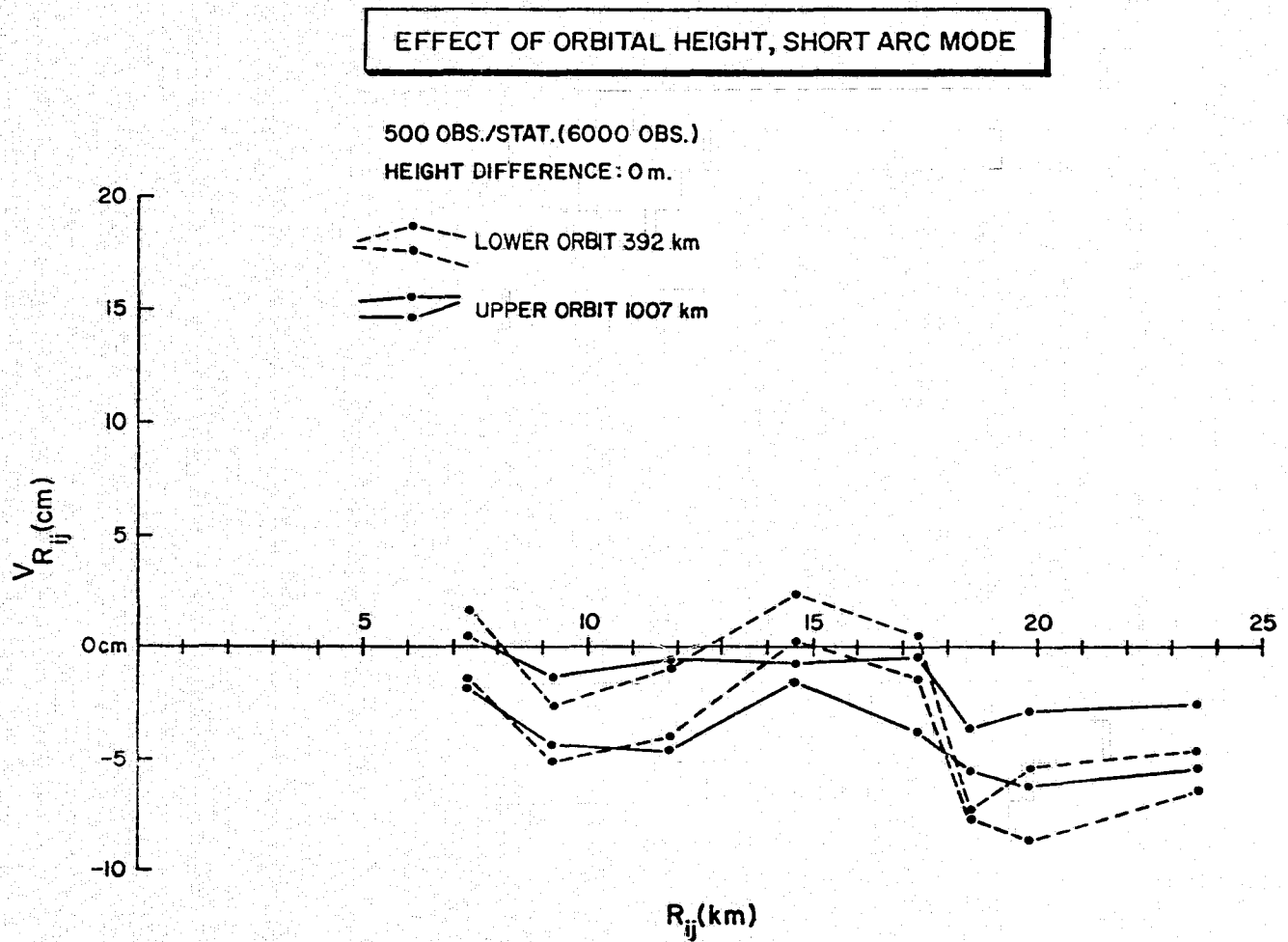
EFFECT OF ORBITAL HEIGHT, SHORT ARC MODE
500 OBS./STAT.(6000 OBS.)
HEIGHT DIFFERENCE: 0 m.
LOWER ORBIT 392 km
UPPER ORBIT 1007 km
20
15
10
5
0cm
-5
-10
$V_{R_{ij}}$(cm)
5
10
15
20
25
R_{ij}(km)

Fig. 5.1-3

consideration in the geometric mode. If the configuration is near critical, the number of observations does not help; on the other hand, if the configuration is not critical, a very low number of observations per station (20-50) can suffice for obtaining an efficiency factor of 1.

5.2.2 Short Arc Mode

The effect of the number of observations per station seemed to be negligible according to Table 5.2-1 and Figures 5.2-1 and 5.2-2. However, an increase in the number of observations seems to make the systematic effects more pronounced due to modeling deficiencies (see Figures 5.2-1 and 5.2-2).

Increasing the number of observations per station could be advantageous if one would like to model these systematic effects. The problem of systematic effects is discussed further in section 5.6.2.

5.3 Number of Fundamental Stations

5.3.1 Geometric Mode

One of the alternatives to break critical configurations was to observe either the distant fundamental stations (future Lageos stations) or other grid stations outside of the small area of investigation. From Tables 5.3-1 and 5.3-2 it appears that at least three fundamental stations need to be observed simultaneously, which may be a very unrealistic requirement. Although one or two fundamental stations look favorable when looking at the standard deviations (Table 5.3-1), Table 5.3-2 shows that due to high correlation the interstation distances could not be recovered with high accuracy in these two cases. It should be kept in mind that in the combination mode (airplane and satellite) no fundamental stations need to be observed to obtain the same or higher accuracy than in the 9 + 3 mode as depicted in Table 5.3-2.

Table 5.2-1

Effect of Number of Events, Short Arc Mode

#	Orbit	Case	Fundamental Stations per Pass	Grid Stations per Pass	Days	Observations per Station				σ_r (cm)	Results	
						Passes	Minimum Events per Pass	Total Observations per Station	Total Observations		Residuals in cm	Spread cm
5	upper	A	3	9	3	9	8	239	2868	10	10 <Δx< 15 2 <Δy< 8 - 34 <Δz< - 29 - 7 <Δr< 2	5 6 5 9
2	upper	A	3	9	3	9	15	483	5796	10	4 <Δx< 7 1 <Δy< 7 - 37 <Δz< - 31 - 6 <Δr< 0	3 6 6 6
3	upper	A	3	9	5	16	15	969	11628	10	3 <Δx< 7 - 4 <Δy< 3 - 43 <Δz< - 37 - 7 <Δr< 1	4 7 6 8
8	lower	A	3	9	5	7	10	254	3048	10	39 <Δx< 51 81 <Δy< 99 -160 <Δz< -143 - 9 <Δr< 1	12 18 17 10
10	lower	A	3	9	5	7	29	758	9096	10	36 <Δx< 51 79 <Δy< 98 -163 <Δz< -147 - 9 <Δr< 2	15 19 16 11

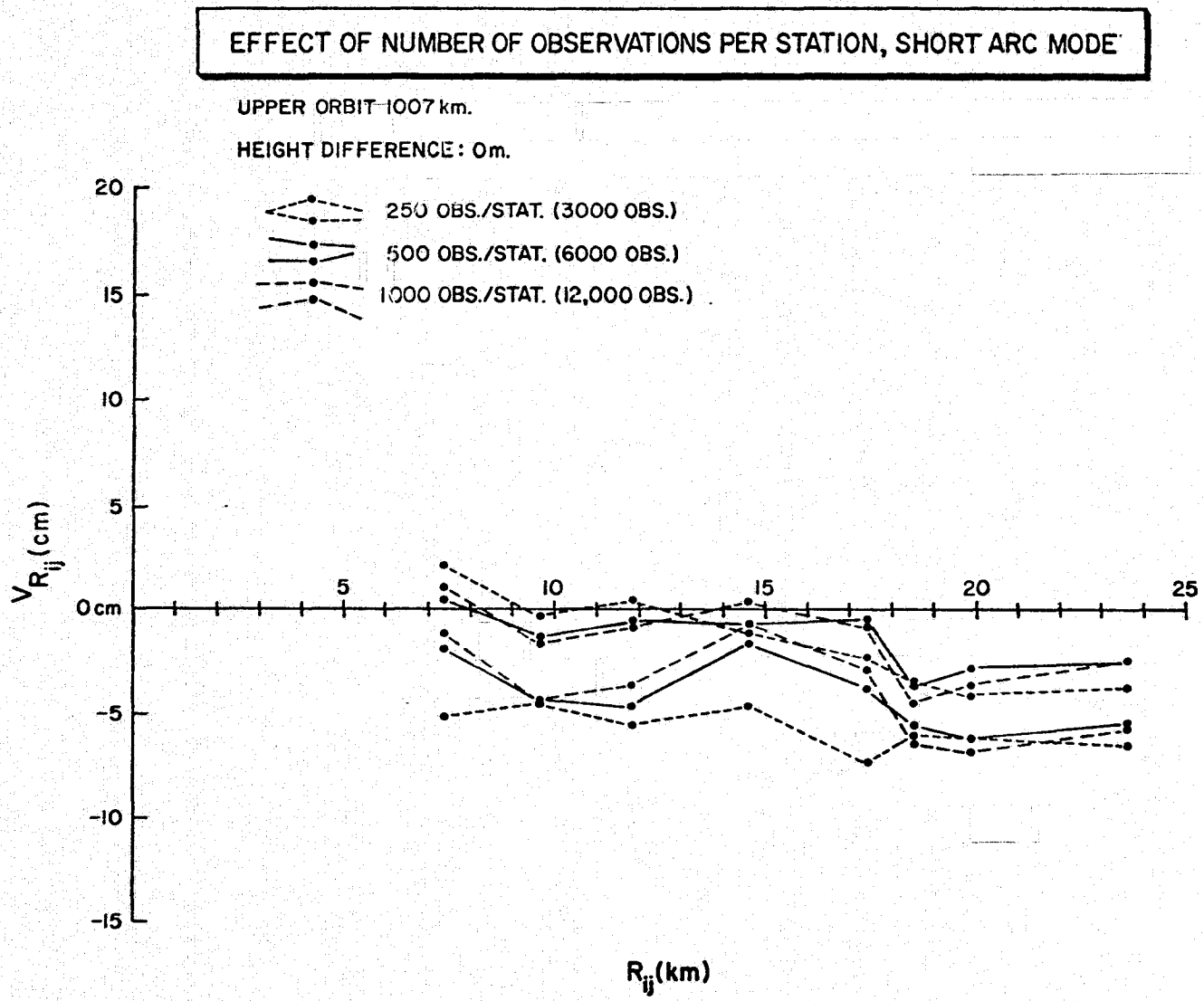
EFFECT OF NUMBER OF OBSERVATIONS PER STATION, SHORT ARC MODE
UPPER ORBIT 1007 km.
HEIGHT DIFFERENCE: 0m.
250 OBS./STAT. (3000 OBS.)
500 OBS./STAT. (6000 OBS.)
1000 OBS./STAT. (12,000 OBS.)
20
15
10
5
0 cm
-5
-10
-15
5
10
15
20
25
$V_{R_{ij}}$ (cm)
R_{ij} (km)

Fig. 5.2-1

EFFECT OF NUMBER OF OBSERVATIONS PER STATION, SHORT ARC MODE

LOWER ORBIT 392 km.

HEIGHT DIFFERENCE : 0 m.

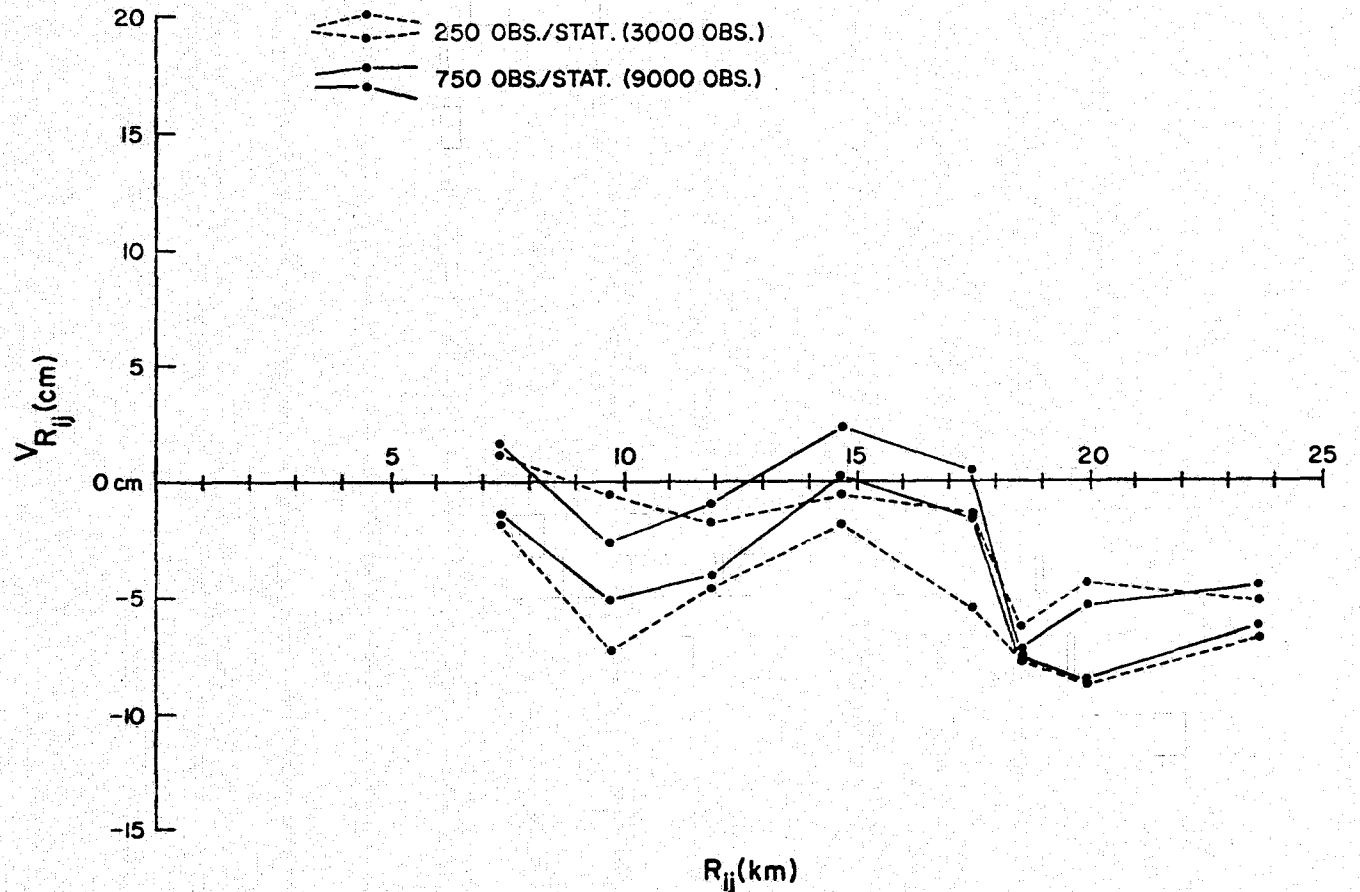

Fig. 5.2-2

Table 5.3-1

Upper Orbit, 500 Observations per Station
Case A (ΔH = 0 m)

Grid Stations + Fundamental Stations	$\sigma_{r_{12}}$ cm	$\sigma_{r_{12}}/r_{12}$ ppm	$\sigma_{\alpha_{253}} \times 10^{-6}$ rad	$\sigma_{\beta_{456}} \times 10^{-6}$ rad
9 + 0	238	325.7	268.1	5.8
9 + 1	3	4.0	4.5	2.3
9 + 2	2	3.2	4.0	2.8
9 + 3	1	1.7	1.4	2.8

Table 5.3-2

Percentage of Residuals (Absolute)

	Residual	0 - 1 cm	1 - 2 cm	2 - 3 cm	3 - 4 cm	>4 cm	Max. Res.
Grid Stations + Fundamental Stations	9 + 0	--	--	--	--	100	669 cm
	9 + 1	28	16	14	14	28	11 cm
	9 + 2	8	17	11	8	56	14 cm
	9 + 3	72	22	6	--	--	3 cm

5.3.2 Short Arc Mode

In contrast to the geometric mode, it was found that short arc solutions with less than three fundamental stations were unable to recover relative station positions satisfactorily. The only option left was to investigate whether or not it was really necessary to observe the three fundamental stations in each pass. Unfortunately, when two fundamental stations were observed per pass there was a rapid decrease in the ability of relative station position recovery (see Figure 5.3-1). This means that unfavorable weather conditions

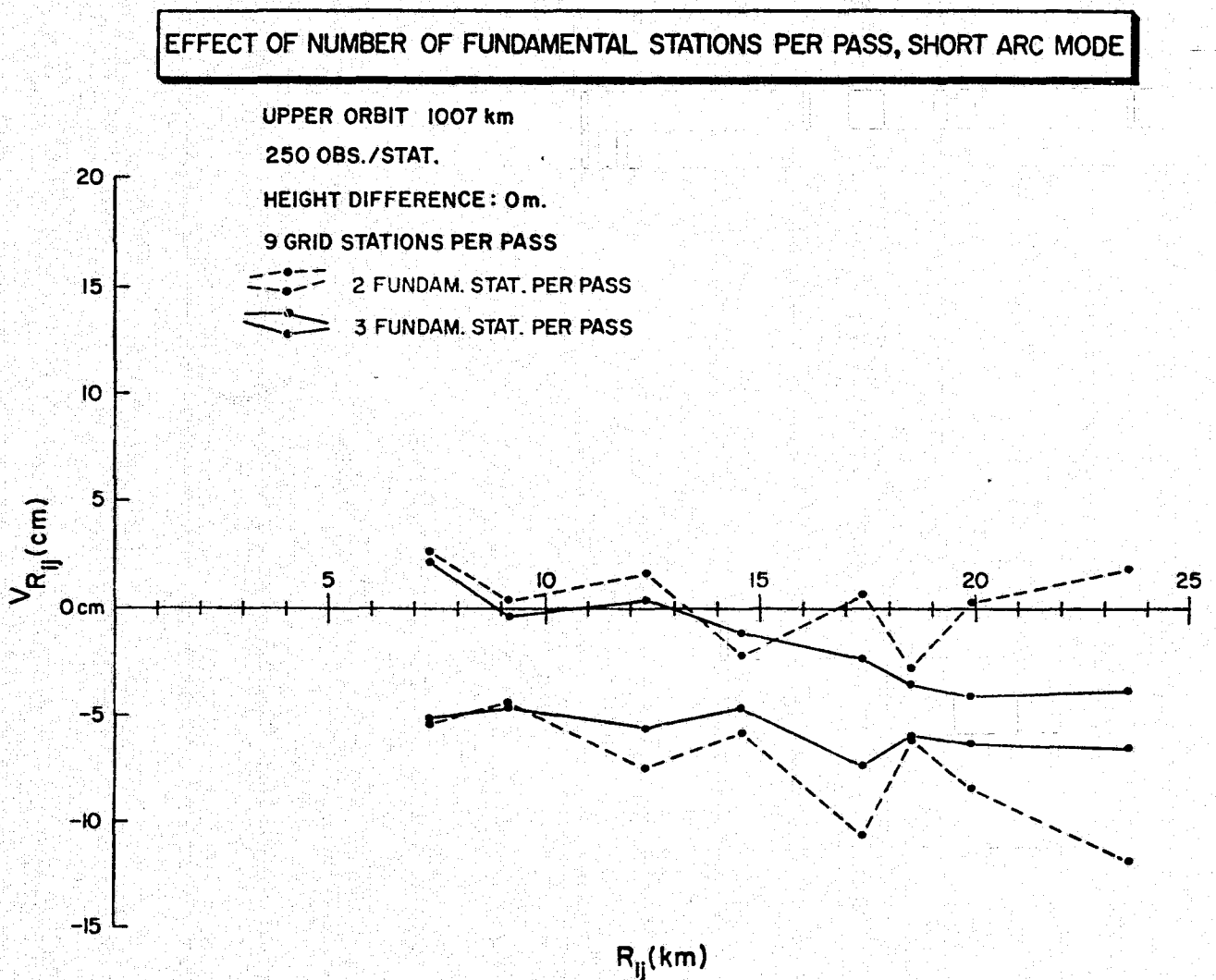
EFFECT OF NUMBER OF FUNDAMENTAL STATIONS PER PASS, SHORT ARC MODE
UPPER ORBIT 1007 km
250 OBS./STAT.
HEIGHT DIFFERENCE: 0 m.
9 GRID STATIONS PER PASS
2 FUNDAM. STAT. PER PASS
3 FUNDAM. STAT. PER PASS
20
15
10
5
0 cm
-5
-10
-15
5
10
15
20
25
$V_{R_{ij}}$(cm)
R_{ij}(km)

Fig. 5.3-1

are as influential in the short arc mode as in the geometric mode. In this case the only advantage of the short arc mode is the absence of the requirement of simultaneous observations.

5.4 Height Difference Between Grid Stations

5.4.1 Geometric Mode

Since the situation of station positions near a plane form a near critical configuration for ranging measurement systems, the extent to which a solution (i.e., the inverse of the normal matrix) might be improved by moving some grid stations out of the plane was investigated. Having height differences of only 100 m (Case B) already showed an improvement. When the height difference was 1000 m (Case C) (See Tables 4.1-1, 5-2, 5.4-1 and 5.4-2), further improvements were evident. For example, in case of the upper orbit, the standard deviation of the distance between stations 1 and 2 dropped from 2.38 m (Case A) to 39 cm (Case B) to 4 cm (Case C). However, from Table 5.4-2 it

Table 5.4-1

500 Observations per Station	Case	$\sigma_{r_{12}}$ cm	$\sigma_{r_{12}}/r_{12}$ ppm	$\sigma_{\alpha_{253}} \times 10^{-6}$ rad	$\sigma_{\beta_{456}} \times 10^{-6}$ rad
lower 392 km	A	290	396.2	277.2	13.8
	B	54	73.7	51.9	6.6
	C	6	8.1	5.6	4.5
upper 1007 km	A	238	325.7	268.1	5.8
	B	39	52.8	47.2	4.1
	C	4	5.6	5.1	3.6

should be noted that the improvement in recovery is not sufficient due to the large correlation which remains even when the stations differ 1000 m in height. Residuals as large as 25 cm are still left between the grid stations. The

creation of height differences in any case is an unrealistic suggestion because the topography in most areas may prove to be unsuitable.

Table 5.4-2

Percentages of Residuals (Absolute)

500 Observations per Station	Case	0 - 1 cm	1 - 2 cm	2 - 3 cm	3 - 4 cm	>4 cm	Max. Res.
lower 392 km	A	--	--	--	--	100	1326 cm
	C	6	8	6	11	69	19 cm
upper 1007 km	A	--	--	--	--	100	669 cm
	C	14	11	11	11	53	25 cm

5.4.2 Short Arc Mode

The nature of the dynamic mode is such that critical configurations due to the fact that stations are situated in or near a plane do not exist as Table 5.4-3 and Figure 5.4-1 show.

Table 5.4-3

Percentage of Residuals (Absolute)
500 Observations per Station, Upper Orbit

Case	0 - 1 cm	1 - 2 cm	2 - 3 cm	3 - 4 cm	>4 cm	Max. Res.
A	22	28	14	14	22	7 cm
C	20	11	25	22	22	6 cm

5.5 Observational Mode

5.5.1 Geometric Mode

The geometric mode does not offer any alternative to simultaneous observations.

EFFECT OF HEIGHT DIFFERENCE, SHORT ARC MODE

UPPER ORBIT : 1007 km

500 OBS./STAT.

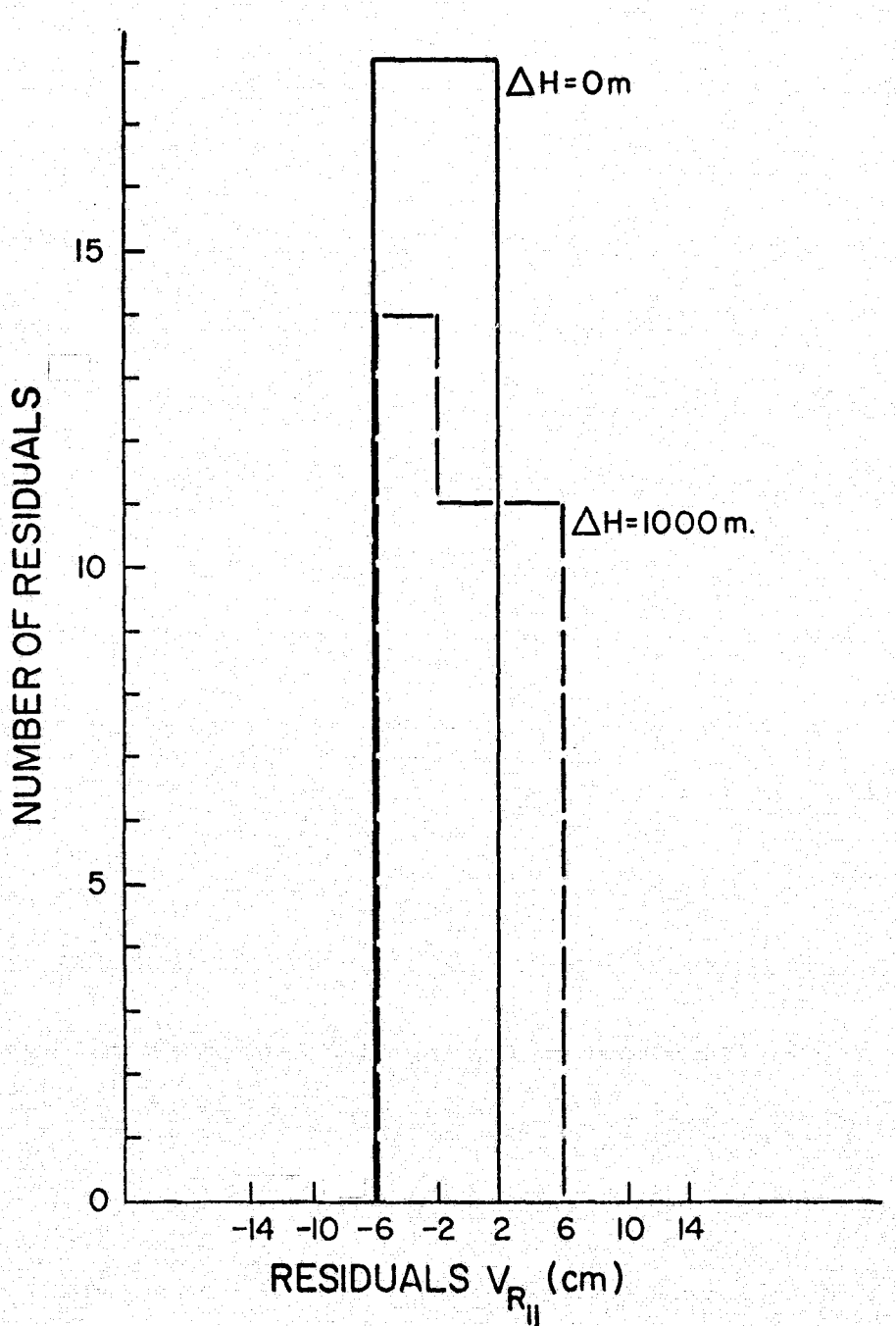

Fig. 5.4-1

5.5.2 Short Arc Mode

Often the ranges used for the short arc mode were the same as those generated for the geometric mode. To ascertain if the simultaneity of the ranges imposed unnecessary constraints on the passes in the short arc mode, similar solutions were made where the simultaneity was broken up.

One example which is shown below originally had one event every 12 seconds, observed by all the 12 (9 + 3) stations. The same solutions with one observation observed to a single station showed hardly any difference. (See Figure 5.5-1 and Table 5.5-1.)

Table 5.5-1

Percentage of Residuals (Absolute)
Upper Orbit, 250 Observations per Station, Case A (ΔH = 0 m)

Mode	0-1 cm	1-2 cm	2-3 cm	3-4 cm	>4 cm	Max. Res.
Simultaneous	11	17	6	19	47	8 cm
Not Simultaneous	11	25	17	22	25	6 cm

5.6 Algorithm

5.6.1 Geometric Mode

The geometric adjustment, which leaves hardly any room for improvement due to its mathematical simplicity, might be investigated in two areas:

(a) Any pitfalls [Pope, 1972] should be avoided in the stepwise adjustment as applied in OSUGOP.

(b) It should be carefully investigated at what stage computational problems due to double precision arithmetic start to dominate the ill-conditioning due to near critical configurations (checks using quadruple precision should be carried out).

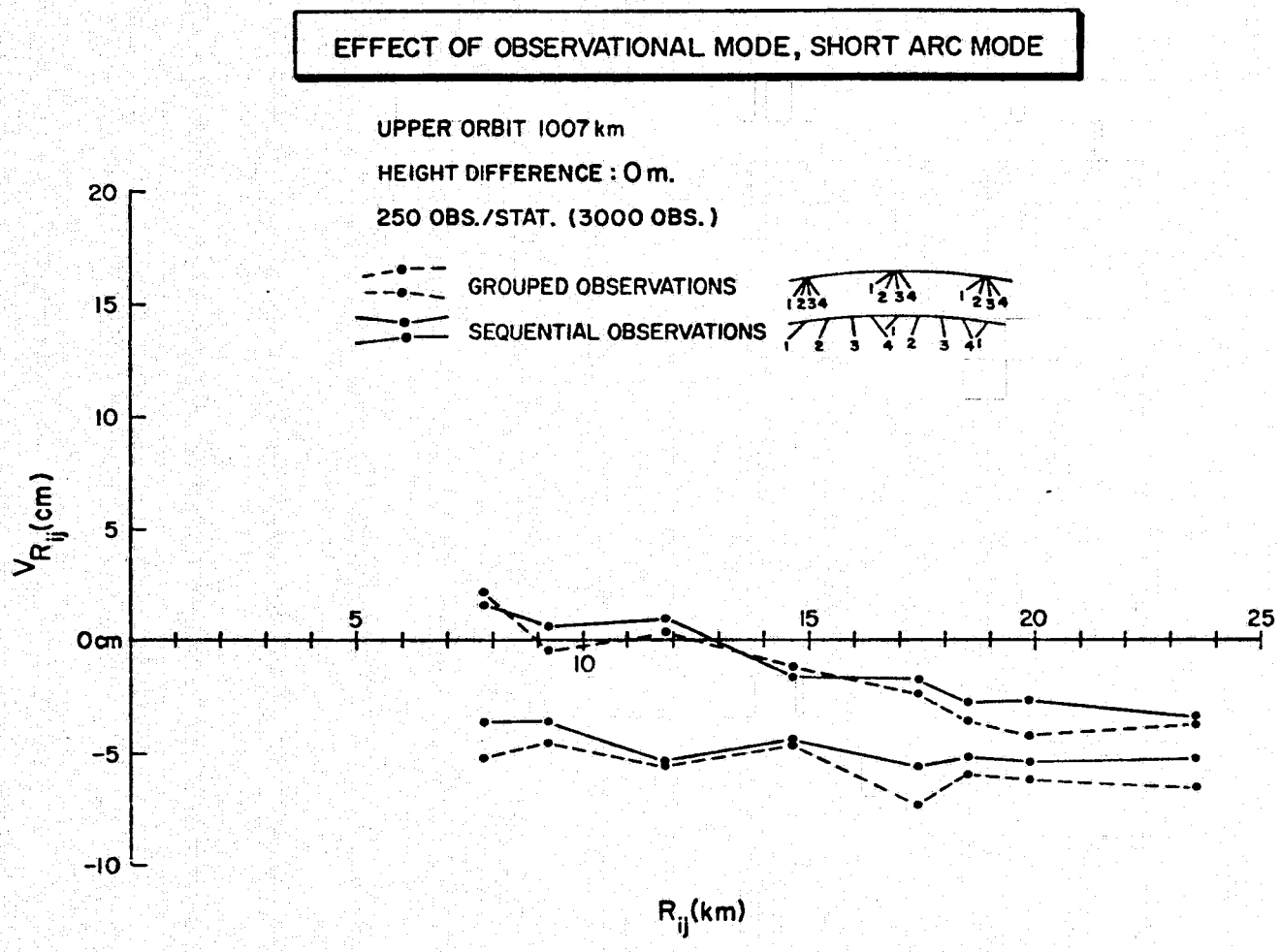
EFFECT OF OBSERVATIONAL MODE, SHORT ARC MODE
UPPER ORBIT 1007 km
HEIGHT DIFFERENCE : 0 m.
250 OBS./STAT. (3000 OBS.)
GROUPED OBSERVATIONS
SEQUENTIAL OBSERVATIONS
1 2 3 4
1 2 3 4
1 2 3 4
1 2 3 4 1 2 3 4 1
20
15
10
5
0cm
-5
-10
5
10
15
20
25
$V_{R_{ij}}$(cm)
R_{ij}(km)

Fig. 5.5-1

5.6.2 Short Arc Mode

5.6.2.1 Gravity Model

As will be explained in section 5.6.2.3, some concern was expressed when solutions with exact ranges (σ = 0 cm) as compared to similar solutions with ranges of σ = 10 cm did not show any improvement in the residuals of the recovered distances between the grid stations. Modeling deficiencies were suspected.

The first possible cause of systematic effects in the residuals of the grid station coordinates could be the difference between the gravity models in the data (orbit) generation program (GTDS) and the solution program (SAGA). To test this hypothesis data was generated with GTDS using only the GEM 6 (15 x 15) gravity field (no drag, etc.). In the solutions the following fields were used:

(a) spherical gravity field (J_0 = 1)

(b) "ellipsoidal" gravity field (J_0, J_2 from GEM 6)

(c) 8 x 8 gravity field from GEM 6

(d) 8 x 8 gravity field as it is inherent in the SAGA program.

The results of the comparison are given in Table 5.6-1.

Table 5.6-1

Percentage of Residuals (Absolute)
Lower Orbit, 250 Observations per Station, Case A (ΔH = 0 m), σ = 10 cm

	0-1 cm	1-2 cm	2-3 cm	3-4 cm	>4 cm	Max. Res.
a	22	6	3	0	69	25 cm
b	25	14	14	8	39	9 cm
c	27	11	17	6	39	9 cm
d	22	22	6	11	39	9 cm

It can be seen that terms beyond J_2 do not give an appreciable improvement. It was concluded that at least the gravity field was not the cause for the large systematic residuals.

5.6.2.2 Nongravitational Forces

Since the gravity field was not the cause of the large residuals, a new lower orbit was generated without any nongravitational forces such as atmospheric drag, solar radiation pressure. Solutions using the truncated GEM 6 (8 x 8) gravity field did not provide any clue as to the nature of the residuals in grid station coordinates (see Table 5.6-2).

Table 5.6-2

Percentage of Residuals (Absolute)
Lower Orbit, 250 Observations per Station, Case A (ΔH = 0 m), σ = 10 cm

	0-1 cm	1-2 cm	2-3 cm	3-4 cm	>4 cm	Max. Res.
Drag, Radiation Pressure	22	22	6	11	39	9 cm
No Drag, No Radiation Pressure	20	19	14	8	39	9 cm

5.6.2.3 Adjustment

The final step which could be made towards the discovery of the reason behind the systematic effects in the residuals of the grid station coordinates was to generate data and solutions with only the GEM 6 (8 x 8) gravity field using either ranges with a standard deviation of 10 cm or true ranges (σ = 0 cm). According to Table 5.6-3, the difference in results is again insignificant. The residuals in terms of grid station coordinates are listed in Table 5.6-4. Subtracting the residuals in X,Y,Z of station 5 from all the others and plotting the differences, clearly shows a very systematic pattern (Fig. 5.6-1).

Table 5.6-3

Percentage of Residuals (Absolute)
Lower Orbit, 250 Observations per Station, Case A (ΔH = 0 m), σ = 0 cm

	0-1 cm	1-2 cm	2-3 cm	3-4 cm	>4 cm	Max. Res.
σ = 10 cm	20	19	14	8	39	9 cm
σ = 0 cm	28	11	8	25	28	8 cm

Table 5.6-4

Station	ΔX (m)	ΔY (m)	ΔZ (m)
1	0.39	0.82	-1.50
2	0.44	0.90	-1.55
3	0.49	0.97	-1.61
4	0.41	0.83	-1.47
5	0.46	0.91	-1.52
6	0.51	0.99	-1.57
7	0.43	0.84	-1.44
8	0.48	0.92	-1.49
9	0.52	1.00	-1.54

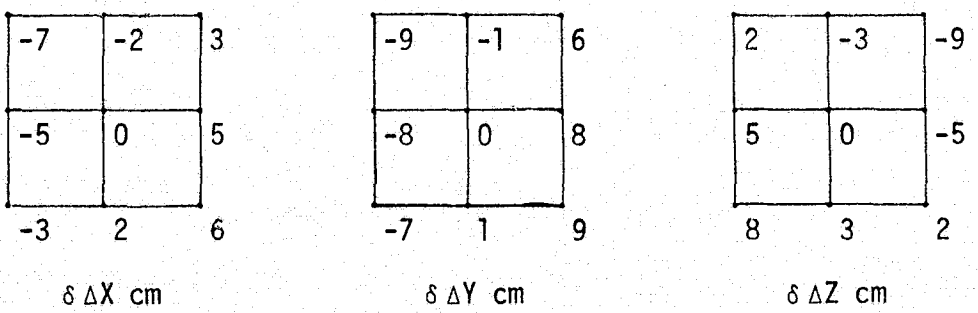

Fig. 5.6-1

Figure 5.6-1 indicates that the distances between the grid stations were not recovered. This implies that the systematic residuals above cannot be described by a similarity transformation but by an affine transformation.

It might also be added that the recovered state vectors (X, Y, Z, $\dot{X}$, $\dot{Y}$, $\dot{Z}$) by the short arc adjustment as compared to the true state vectors, in a body-fixed system, show residuals in $\dot{X}$, $\dot{Y}$ which are a factor of 100 larger than the residuals in X, Y, Z, $\dot{Z}$. In an inertial system the residuals in X, Y are a factor of 100 larger than the residuals in Z, $\dot{X}$, $\dot{Y}$, $\dot{Z}$. This clearly indicates a rotational problem, namely, the corrections to $\dot{X}$, $\dot{Y}$ were such that in a body-fixed system the polar orbit did not yield tracks of subsatellite points which form an angle with the meridians (at the equator the angle is about 3°.5).

The reasons for the above problems are not clear at the present time.

6. SUMMARY AND CONCLUSIONS

The Close Grid Geodynamic Measurement System was conceived as an orbiting ranging device with a ground base grid of reflectors or transponders (spacing 0.5 - 50 km), which are projected to be of low cost (maintenance free and unattended), and which will permit the saturation of a local area to obtain data useful for geodynamic and geodetic (oceans included) purposes. In this investigation a first attempt was made to get an insight on how maximum accuracy of relative station positions can be achieved in a short time span (3-5 days).

Measurement systems as laser radar, RF radar or a combination of both operating in continuous wave or pulse mode are able to provide ranges, range rates (Doppler) or range differences (integrated Doppler). In this study only ranges were considered with the already feasible laser precision of 10 cm. The ranges are observed in two modes, simultaneous and nonsimultaneous. Two types of vehicles carrying the transmitter have been considered: (A) Satellites at various altitudes: 392, 657 and 1007 km. The satellite orbits (passes) were generated with the Goddard Trajectory Determining System (GTDS), developed at NASA's Goddard Space Flight Center. (B) Airplane flying at an altitude of 9 km.

Two types of stations were considered: (A) Nine grid stations at five-minute intervals chosen in the vicinity of the San Andreas Fault area in California ($\Delta\phi$ = 9.3 km and $\Delta\lambda$ = 7.3 km). The ellipsoidal height differences between the stations were varied between 0 and 1000 m. (B) Three distant fundamental stations were selected outside the grid area near San Diego and Quincy in California and near Bear Lake, Utah.

Having simultaneous and nonsimultaneous ranges, two different algorithms can be used to compute the relative positions of grid stations: (A) Geometric

adjustment which takes advantage of the simultaneity of the observations. The software used was The Ohio State University Geometric and Orbital (Adjustment) Program for Satellite Observations (OSUGOP). (B) Short arc adjustment (dynamic mode) which does not have the requirement of simultaneous observations. The software used was the Short Arc Geodetic Adjustment Program (SAGA). Since a range measurement system lacks any coordinate system definition, especially in the geometric mode, the recovery of the relative positions was expressed in terms of the estimable quantities, the lengths of the chords between the grid stations and the angles between the chords.

6.1 Geometric Mode Results

The geometric mode leads to a very simple mathematical model. However, local satellite ranging networks often degenerate into critical configurations (see Table 6-1, line 1) as opposed to global satellite ranging networks. To avoid these critical configurations two possibilities are mentioned: (1) Separate stations in height either by giving the grid stations some height difference ΔH (Table 6-1, line 2), a possibility only in the case of accommodating topography, or by including into the observation campaign the three stations outside the area (Table 6-1, line 4). This possibility has the stringent requirement of having favorable weather conditions at the different sites (grid area and 3 fundamental stations). (2) Separate the ranging devices in height. The best (and most realistic) solution to avoid the effects of critical configurations within the limited area of the grid is the combination of an airplane and a satellite (Table 6-1, line 5. Note that no distant [fundamental] stations are needed.) The only disadvantage of geometric mode is the instrumental problem related to the realization of the simultaneous observations. These at least for the lasers may be overwhelming.

Table 6-1

RECOVERY OF STATION-TO-STATION DISTANCES

36 Distances Between 9 Grid Stations, 500 Observations per Station
Accuracy of Range Measurements: σ_r = 10 cm

	Mode	ΔH (m)	No. of Grid Stations	No. of Fundamental Stations	Height (km)		Percentages of Residuals (Absolute)					
					Satellite	Airplane	0-1 cm	1-2 cm	2-3 cm	3-4 cm	>4 cm	Max. Res.
	Geometric	0	9	0	1007	--					100	669
Alternatives	Geometric	1000	9	0	1007	--	14	11	11	11	53	25
	Geometric	0	9	1	1007	--	28	16	14	14	28	11
	Geometric	0	9	3	1007	--	72	22	6			3
	Geometric	0	9	0	392	9	69	28	3			3
	Short Arc	0	9	3	1007	--	22	28	14	14	22	7

6.2 Short Arc Mode Results

The absence of the requirement of having simultaneous observations and the absence of the bothersome critical configurations are the main advantages of the short arc mode. However, in order to get stability in the solutions, the three distant (fundamental) stations must be observed during each pass (Table 6-1, line 6). A pass of four- to ten-minute lengths for satellites at altitudes between 400 and 1000 km is so short in duration that favorable weather conditions occurring simultaneously at all the sites might be just as stringent a requirement as in the case of the geometric mode. (Short arc mode using RF radar may alleviate the weather dependency but is negatively compensated by more serious refractional problems and more complex active grid stations.)

The information contained in Table 6-1 has also been graphically represented within Figure 6-1 to bring out the comparison between various approaches.

6.3 Conclusions

Ranging with σ_r = 10 cm and 500 observations per station can recover relative positions well ($\sigma_{r_{ij}}$ = 4 cm and $|v_{r_{ij}}| < 3$ cm). Unit efficiency $\sigma_r/\sigma_{r_{ij}}$ can be achieved with fewer observations. Expected improvements in the ranging accuracy (to 1-2 cm) and in the corresponding precision makes the proposed system an excellent candidate for geodetic and geodynamic applications. As far as the mode of operation is concerned for a laser system, the following trade-offs need to be considered: The likelihood of having favorable weather conditions at the distant sites in case of the short arc mode (possibly with a single satellite and nonsimultaneous ranging)

RECOVERY OF STATION-TO-STATION DISTANCES

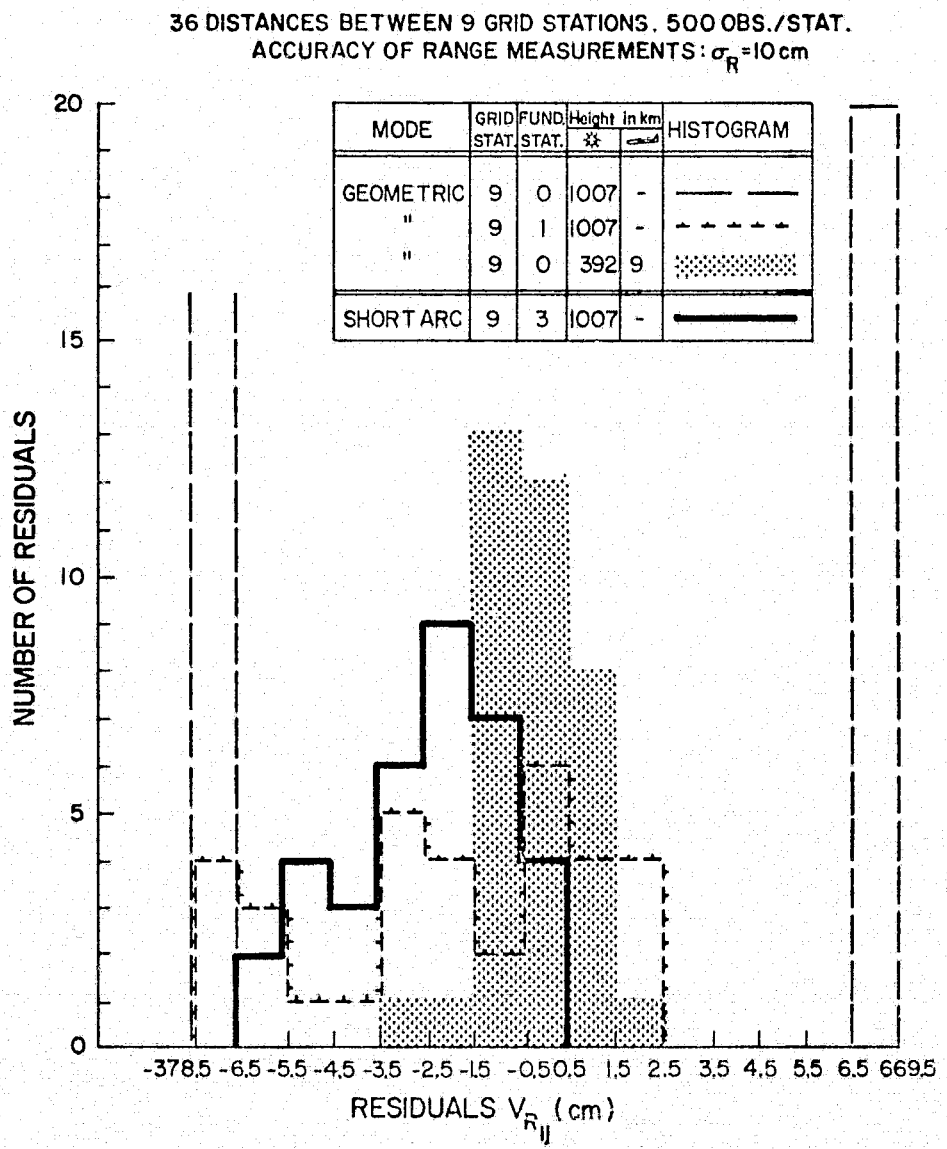

Fig. 6-1

versus the feasibility of overcoming instrumental problems in the geometric mode (airplane and satellite with simultaneous ranging).

Neither of these problems are critical for an RF system, and the decisive factor is whether systematic errors affecting the RF systems can be reduced to the level of those required by the users of the system.

6.4 Applications

Possible candidates as users of a Close Grid Geodynamic Measurement System are: Solid Earth--measurement of motions near plate boundaries, subsidence and uplift, regional strain measurements, horizontal motions and dilatancy components near faults, post earthquake resurvey, regional tidal loading, volcanism associated motions, surface motions on unstable slopes, geodetic surveys. Cold Regions--measurement of rigid body motions, deformations and strains associated with the dynamics of pack ice and ice islands, snow/ice motions in major ice sheets, profile and flow of glaciers, surface motions in permafrost. Marine Geodesy--positioning of ocean bottom geodetic reference frame, positioning or tracking of surface buoys.

7. RECOMMENDATIONS FOR FUTURE STUDIES

A. The grid station network should be extended to a large grid (1000 stations). Organization of observations might be a major task in this case.

B. Once a large network has been set out, measured and recovered, actual changes in the relative positions of the grid stations should be simulated. A second recovery adjustment will give an insight in the capabilities of monitoring these changes in relative position.

C. Better algorithms for short arc adjustment should be devised to remove systematic effects at the centimeter level.

D. A short investigation should be made into the correctness of the step and iterative adjustment procedure and the computational accuracy of geometric mode algorithms.

E. An optimum estimation procedure for station recovery might be a geometric mode which takes advantage of orbital constraints which connect the different (unknown) satellite positions, or, the reverse, a short arc mode which makes use of (near) simultaneities between observations.

F. The case of very closely spaced (< 1 km) grid system should be investigated because of numerous potential applications to engineering works.

REFERENCES

Aardoom, L. 1972. "Geometric Accuracy Obtainable from Simultaneous Range Measurements to Satellites," Geophysical Monograph, 15. Edited by S.W. Henriksen, A. Mancini, and B.H. Chovitz, American Geophysical Union, Washington, D.C.

Anderle, R.J. 1974. "Transformation of Terrestrial Data to Doppler Satellite Datum," J. of Geophysical Research, 79, 35.

Bjerhammer, A. 1973. Theory of Errors and Generalized Matrix Inverses. New York: Elsevier Scientific Publishing Co.

Blaha, G. 1971a. "Inner Adjustment Constraints with Emphasis on Range Observations." The Ohio State University Department of Geodetic Science Report No. 148.

Blaha, G. 1971b. "Investigations of Critical Configurations for Fundamental Range Networks." The Ohio State University Department of Geodetic Science Report No. 150.

Brown, D.C. and J.E. Trotter. 1969. "SAGA, A Computer Program for Short Arc Geodetic Adjustment of Satellite Observations." AFCRL Report 69-0080. Air Force Cambridge Research Laboratory, Bedford, Mass.

Brown, D.C. and J.E. Trotter. 1973. "Extensions to SAGA for the Geodetic Reduction of Doppler Observations." AFCRL Report No. AFCRL-TR-73-0177. Air Force Cambridge Research Laboratory, Bedford, Mass.

COSMIC. 1974. (Computer Software Management and Information Center). Operating Manuals, Vols. 1 and 2. Document ID No. 0013763, University of Georgia, Athens.

Drake, C.L., O.L. Anderson, C.A. Burk, A.V. Cox, J.R. Goldsmith, L. Knopoff, J.C. Maxwell, F. Press, E.M. Shoemaker, T.H. Van Andel and P.J. Hart. 1973. U.S. Program for the Geodynamic Project, Scope and Objective. National Academy of Sciences, Washington, D.C.

Escobal, P.R., K.M. Ong, O.H. von Roos, M.S. Shumate, R.M. Jaffe, H.F. Fliegel and P.M. Muller. 1973. "3-D Multilateration: A Precision Geodetic Measurement System." Technical Memorandum 33-605, Jet Propulsion Laboratory, Pasadena, Calif.

Gaposchkin, E.M. 1973. "1973 Smithsonian Standard Earth (III)." SAO Special Report 353. Smithsonian Astrophysical Observatory, Cambridge, Mass.

Grafarend, E. and B. Schaffrin. 1974. "Unbiased Free Net Adjustment," Survey Review, XXII, 171.

Hartwell, J.G. 1968. "A Theoretical Development for the Determination of the Center of Mass of the Earth From Artificial Satellite Observation." Paper presented to 49th Annual Meeting of the AGU, Washington, D.C.

Hartwell, J.G. and T.R. Lewis. 1967. Integration of Orbits and Concomitant Variational Equations by Recurrent Power Series. Duane Brown Assoc.

Krakiwsky, E.J. and A.J. Pope. 1967. "Least Squares Adjustment of Satellite Observations for Simultaneous Directions or Ranges." The Ohio State University Department of Geodetic Science Report No. 86.

Meissl, P. 1969. "Zusammenfassung und Ausbau der inneren Fehlertheorie eines Punkthaufens." In Karl Rinner, Karl Killian, Peter Meissl, "Beitrage zur Theorie der geodatischen Netze im Raum," Deutsche Geodatische Kommission, Reihe A., 61.

Mueller, Ivan I. 1967. "Data Analysis in Connection with the National Geodetic Satellite Program." The Ohio State University Department of Geodetic Science Report No. 93.

Mueller, Ivan I. 1968. "Global Satellite Triangulation and Trilateration," Bulletin Geodesique, 87.

Mueller, Ivan I., J.P. Reilly, C.R. Schwarz, and G. Blaha. 1970. "SECOR Observations in the Pacific." The Ohio State University Department of Geodetic Science Report No. 140.

Mueller, Ivan I., M. Kumar, J.P. Reilly, N. Saxena, and T. Soler. 1973. "Global Satellite Triangulation and Trilateration for the National Geodetic Satellite Program." The Ohio State University Department of Geodetic Science Report No. 199.

Mueller, Ivan I. 1975. "Tracking Station Positioning from Artificial Satellite Observations," Geophysical Surveys. In press.

Pope, A.J. 1972. "Some Pitfalls to Be Avoided in the Iterative Adjustment of Nonlinear Problems." Proceedings of the 38th Annual Meeting, American Society of Photogrammetry, Washington, D.C., March 12-17.

Rao, C.R. 1973. Linear Statistical Inference and Its Applications, 2nd Edition. New York: John Wiley, Inc.

Reilly, J.P., C.R. Schwarz, and M.C. Whiting. 1972. "The Ohio State University Geometric and Orbital (Adjustment) Program (OSUGOP) for Satellite Observations." The Ohio State University Department of Geodetic Science Report No. 190.

Rinner, K. et al. 1969. "Beitrage zur Theorie der Geodatischen Netze im Raum," Deutsche Geodatische Kommission, Reihe A., 61.

Smith, D.E., R. Kolenkiewicz, R.W. Agreen, and P.J. Dunn. 1974. "Dynamic Techniques for Studies of Secular Variations in Position from Ranging to Satellites." GSFC Report X-921-74-161, Goddard Space Flight Center, Greenbelt, Md.

Tsimis, E. 1972. "On the Geometric Analysis and Adjustment of Optical Satellite Observations." The Ohio State University Department of Geodetic Science Report No. 185.

Tsimis, E. 1973. "Critical Configurations (Determinantal Loci) for Range, and Range-Difference Satellite Networks." The Ohio State University Department of Geodetic Science Report No. 191.

Uotila, U.A. 1967. Introduction to Adjustment Computations with Matrices. Lecture Notes. The Ohio State University Department of Geodetic Science.

Wagner, W.E. and C.E. Valez, (Eds.) 1972. "GTDS Mathematical Specifications." GSFC Report X-552-72-244, Goddard Space Flight Center, Greenbelt, Md.

Weiffenbach, G.C. 1973. Use of a Passive Stable Satellite for Earth-Physics Applications. Final Report prepared under Grant NGR 09-015-164 for National Aeronautics and Space Administration, Washington, D.C.